Published in final edited form as:
Adv Drug Deliv Rev. 2012 December ; 64(15): 1800–1819. doi:10.1016/j.addr.2012.05.008.

Biocompatibility Assessment of Si-based Nano- and Micro-particles

Hamsa Jaganathan[a] and **Biana Godin**[a,*]
[a]Department of Nanomedicine, The Methodist Hospital Research Institute, Houston, TX

Abstract

Silicon is one of the most abundant chemical elements found on the Earth. Due to its unique chemical and physical properties, silicon based materials and their oxides (e.g. silica) have been used in several industries such as building and construction, electronics, food industry, consumer products and biomedical engineering/medicine. This review summarizes studies on effects of silicon and silica nano- and micro-particles on cells and organs following four main exposure routes, namely, intravenous, pulmonary, dermal and oral. Further, possible genotoxic effects of silica based nanoparticles are discussed. The review concludes with an outlook on improving and standardizing biocompatibility assessment for nano- and micro-particles.

Keywords

silicon; silica; nanomaterials; biocompatibility; toxicity; mesoporous

1. Introduction

This review summarizes continuing efforts in understanding the factors affecting biocompatibility of silicon-based nano- and micro-scale materials. Silicon, or Si, is one of the most abundant chemical elements found on the Earth.[1] Its oxide forms, such as silicate (SiO_4) and silicon dioxide, also known as silica (-SiO_2-), are the main constituents of sand and quartz contributing to 90% of the Earth's crust. Due to its unique chemical and physical properties, Si based materials have been used in several industries such as building and construction, electronics, food industry, consumer products and biomedical engineering/medicine. In building and construction Si-based materials are used for the production of concrete, glass, sealants and lubricants[2]. In the electronics industry, Si is one of the predominant elements, and is used as a substrate for integrated circuit chips found in computers, cell phones and other electronic devices.[3] In the food industry, silica (SiO) serves as a preservative and thinning agent. Si based products are also widely utilized for biomedical applications. As an example, Si and SiO based materials are used for decades in dietary supplements[4], bandages[5], catheters and implants[5], dental fillers[6] and contact lenses[5]. Since these macroscopic devices are known to be generally safe and biocompatible, a number of Si and SiO based consumer over-the-counter products with nano/micro-scale particles were developed. As an example, Nanoceuticals™ Microbright

*Correspondence: bgodin@tmhs.org, phone number: 713-441-7329, fax number: 713-441-7834 .

Tooth Powder, made out of silica-mineral hydride, contains nanoscaled molecular cages (1 – 5 nm diameter) that can cleanse teeth by reducing the residing acidity from food particle compounds. SiO based nano- and micro-scaled materials[7] are also used in dietary supplements to increase absorption of nutrients in the body (www.nanotechproject.org). Furthermore, intensive investigations on the use of Si based nano- and micro-materials for improved delivery of therapeutics and imaging agents to a number of conditions affecting various body systems are being conducted worldwide by numerous research groups. Si based materials have been investigated as a vehicle for drug delivery for the past few decades.[8] Si element exhibits a vast array of different chemistries, in which size, shape, and surface of the nano- and micro-structures can be easily manipulated depending on the desired properties as a drug carrier.[9] Encapsulation of enzymes, bacteria, and mammalian cells in amorphous SiO nano- and micro-particles demonstrated a prolonged shelf life and no change in their metabolic activities, indicating the high potential of Si based particles for improved delivery of bioactive substances.[10]

It is known that materials on a sub-micron and micron scale possess characteristics that can impose their biological behaviors. Thus, it is necessary to understand the short and long-term effects and potential hazards from nanomaterials as they are exposed to the human body and the environment. Moreover, nanotoxicity, or the toxicity induced by nanomaterials, to humans is becoming a great concern as more and more consumer products embedded with nanomaterials are used without regulation.[11] Although agencies[12], such as Food and Drug Administration (FDA) and the National Institute of Standards and Technology (NIST), have initiated programs to control the usage of nanomaterials for manufacturing consumer products, there are a number of world-wide companies that have stated there is a nanotechnology component in their already marketed products (www.nanotechproject.org). Compared to Materials Safety Data Sheets (MSDS), which are a set of documents stating the handling procedures and potential hazards for chemical compounds, it is generally difficult to predict and standardize the health and environmental effects from nanomaterials. This difficulty is due to numerous methods and manipulations that can be performed to design nanomaterials as well as due to the specific interaction the nanomaterial can have with the cells in living organism. For example, the aggregation behavior for amorphous SiO particles can be altered at different particle sizes (30 and 80 nm in diameter).[13] Larger NPs aggregate quickly, whereas, smaller NPs aggregate slowly at high ionic strengths of the solution. This dependence of NP size on aggregation states is important especially in the human body, when physiological pH levels, ionic strength and temperatures of body fluids can alter the behavior and function of delivered NPs. Along with size, the geometry of the nanostructure can govern a NP's behavior in the body. As an example, short-rod (aspect ratio 1.5) mesoporous SiO NPs were found in the liver and long-rod (aspect ratio 5) mesoporous SiO NPs were found in the spleen after being intravenously administered to mice.[14] These particulates exhibited different clearance rates due to an alteration in the shape. The modulation of NP surface charge can affect cellular uptake as well.[15] These examples of different biological responses based on the physico-chemical characteristics of the particles, indicate the critical need to realize that toxicity from nano- and micro-particles is a multi-factorial process which is difficult to predict. Thus, it becomes challenging to categorize the health and safety outcomes for each type of nanomaterial. Though Si-based nanomaterials are widely used in various industries, the long-term effects of their exposure to humans and the environment are unclear (similarly to the majority of other nanomaterials). In this review, we summarize the ongoing research efforts in understanding the potential outcomes after Si-based nanomaterial exposure. The manuscript launches with a brief overview on the chemistry and fabrication methods of Si-based nano- and micro-materials. In the following sections, *in vitro* and *in vivo* studies of Si-based particles exposure through different drug administration routes, namely intravenous injections, pulmonary inhalation, dermal application and gastrointestinal intake (Fig. 1), are

reviewed. Lastly, the underlying concern of potential genotoxicity, or the toxicity induced at the DNA level, due to Si based nanomaterials is discussed.[16]

2. Chemistry and Fabrication of Si based Particles

2.1.Silicon vs. Carbon

Si chemistry is very diverse as discussed by many reviews and books.[17-20] Nanoscale fabrication using Si materials is relatively more complex than using carbon (C), an element from the same Periodic Table group (Group IV) as silicon. Due to the ability to form four bonds, a vast array of chemical structures can be created for both elements. This similarity of Si to C was used by several Science fiction authors to describe other forms of life based on Si. The most famous examples are Herbert Wells's writing about Silicon based life and a Si-based alien which appeared in one of the *Star Trek* episodes *"The Devil in the Dark".*

Generally, carbon nanomaterials (i.e. single walled and multi walled carbon nanotubes) have a low likelihood in serving as drug delivery carriers due to concerns of non-biodegradability and the fact that they retain in the body tissues, causing toxic effects as evidenced from *in vitro* and *in vivo* studies[21-26]. On contrary, since Si-Si and Si-O bonds are weaker than correspondent C-C and C-O ponds, Si-based materials are biodegradable and thus considered more biocompatible than carbon-based, but their fabrication is generally more challenging. Though Si has the same number of electrons in its outer shell, carbon and silicon exhibit very different structural, chemical, and physical properties, making the fabrication of nano- and micro-materials based on these elements dissimilar.[27]

One reason for the difference between Si and C is the electronegativity. The electronegativity of carbon (χ=2.55) is higher than the electronegativity of hydrogen (χ=2.20), leading to stable, polarized C-H bonds. The electronegativity of silicon (χ=1.9) is lower than carbon and hydrogen, causing Si-H bonds to be polarized in the opposite direction with nucleophilic attacks occurring at the central Si atoms.[28] The Si-Si bonds are also weak (222 kJ mol^{-1}), easily forming new bonds with other elements without affecting crystallinity of nanostructures.[29] In addition, the energy difference between the valence s and p orbitals of carbon and silicon plays an important role in creating strong bonds and effectively constructing nanostructures. The energy difference of Si is 5.66eV, whereas for C, it is 10.60 eV (E_p-E_s).[28] Carbon activates one valence p orbital for sp, sp^2, and sp^3 hybridization (triple, double, and single bonds, respectively), allowing for the synthesis of all different shapes of carbon nanostructures. Conversely, silicon uses all three valence p orbitals for only sp^3 hybridization (single bonds). As a consequence, Si bonds with other elements are longer than those of Carbon (as summarized in Table 1), and, thus, more fragile.

2.2.Fabrication of nonporous Si based particles

Realizing the unique chemical properties of the Si element has aided investigators to fabricate Si nanomaterials. One of the basic criteria for injectable particles for drug delivery is an ability to disperse them in aqueous media and biological fluids.[31] Although there are numerous methods to prepare Si NPs, including thermal vaporization[32], pyrolysis of silane[33, 34], the microwave plasma decomposition method[35], laser-induced decomposition[36-40], these synthesis methods are not compatible for biomedical applications as they use nonpolar organic solvents and often produce hydrophobic surfaces.[28] The first example of Si NPs synthesized from a solution was performed by Heath in 1992.[41] This liquid-solution-phase technique was used for preparing single Si hexagonal-shaped crystals of 5-3,000 nm in size, based on the reduction of $SiCl_4$ and $RSiCl_3$ (R = H, octyl) by sodium metal in a nonpolar organic solvent at high temperatures (385°C) and high pressures (> 100 atmospheres). Other groups reported synthesis of tetrahedral Si

nanocrystals possessing improved optical and electronic properties produced in low temperatures and pressure by sodium naphthalenide reduction of silicon tetrachloride in 1,2-dimethoxyethane followed by surface termination with an excess of *n*-butyl lithium. [42, 43] A few studies have reported the production of water-dispersible Si particles, but these particles do not exhibit an adequate colloidal stability necessary for biological environments. [31]

2.3.Fabrication of Nonporous SiO based Particles

Nanomaterials composed of silica, or SiO, can intrinsically be dispersed in aqueous media. The Stöber method, reverse mircoemulsion, and Sol-Gel process are the three general routes for the synthesis of SiO based NPs. Stöber *et al.* first synthesized SiO NPs with diameter in 200 – 800 nm through hydrolysis and condensation of silicon alkoxides in alcoholic solutions, which is now called the Stöber method.[44] A modified Stöber method was used to fabricate fluorescent and photostable core-shell SiO particles, so called Cornell dots (C-dots) with diameters of 3-30 nm[45]. The near-infrared dye-doped C-dots[46], which due to their small size can pass through glomerular filtration and excreted through kidneys have recently entered Phase I clinical trial. C-dots are aimed being tested for their safety on five melanoma patients.[47] Reverse microemulsion method, developed by Arriagada and Osseo-Asar, can synthesize uniform SiO NPs via water-in-oil techniques.[48, 49]

2.3.1. Sol-Gel Process—Sol-Gel process is probably the most commonly used method for fabrication of SiO based particles. Under mild conditions of low temperature and pressure,[50] SiO particles are synthesized from triethoxysilane (TEOS). The chemical process can be described as follows (Equation 1):

$$\mathrm{Si(OR)_4 + 2H_2O \xrightarrow{H+ \quad or \quad OH-} SiO_2 + 4ROH} \quad (1)$$

The process allows for an accurate control over morphology and surface functionalization by manipulating the water/silane ratio, catalyst, temperature, and the type of solvent. Acid or base catalysis can be performed due to the low reactivity of silicon. In the presence of an acid catalyst, linear growth of the SiO particles would form with sizes below 100 nm. In a base catalyst, large spherical particles can form in the micrometer range.[50] Drugs can easily be loaded into SiO particles during the sol-gel synthesis. Wen *et al.* demonstrated that ibuprofen encapsulated SiO NPs produced a sustained release of drugs in artificial gastric fluid.[51] Aside from encapsulation, the surface of SiO particles can be further functionalized with polymers, such as chitosan[52], aiming at specific biomedical applications. In addition, to using SiO and Si-particles, researchers have also designed SiO as a shell component for multifunctional particles. The high solubility, vast array of functionalization techniques, and biocompatibility make SiO material an advantage surface coating to magnetite[53, 54], gold[55], silver[56], quantum dots[57], and carbon nanotubes[58].

2.4. Fabrication of Porous Si and SiO particles

Porous silicon (pSi) and silica (pSiO) particles have been investigated for the past few decades for drug delivery applications.[59] There are three types of porous structures: nanoporous, mesoporous, and macroporous based on the diameter of the pores. The term “nanoporous” refers to pore diameters of less than 2 nm, “mesoporous” - diameters between 2 and 100 nm and “macroporous” to pore size range of greater than 100nm.[60] Mesoporous pSi and pSiO particles exhibit high surface areas, large pore volumes, tunable pore sizes, and good chemical and thermal stability, making them a suitable candidate for controlled release of drugs.[61]

The discovery of pSi was reported more than 50 years ago by Arthur Ulhir.[62]. Electrochemical anodization is a popular method to fabricate pSi particles by using single crystalline Si wafers in a hydrofluoric acid electrolyte solution. Drugs can be loaded into the pores and protected from the biological environment until the particle arrives to the target site for drug treatment. More than two decades ago, Canham, who worked for Bell industries at that time, first demonstrated that unlike their nonporous counterparts, pSi structures are able to degrade in physiological environments making them especially suitable candidates for drug delivery[63]. The main degradation product of pSi is monomeric silicic acid ($Si(OH)_4$), which is naturally found in bone and other tissues, making pSi particles an effective drug delivery platform. In the Western world, the average daily dietary intake of Si, the essential body mineral, is 20–50 mg [64]. Highly pSi (porosity >50%) dissolves in the majority of the simulated biological fluids including serum and PBS, except for the acidic environment such as the simulated gastric fluid [59]. It was also shown that the biodegradation of pSi structures is dependent on the porosity and the surface modifications[65]. Since then numerous reports in this field have been published. The focus of the majority of these studies was on *in vitro* interactions of pSi structures with biological substances, such as biodegradation in physiological conditions[65], calcification [66], cell adhesion [67], interaction with neuron interfaces and neural networks [68] and protein adsorption [69].

Several studies demonstrated that pSi or pSiO particles can release drugs in a controlled manner through a combination of passive diffusion and degradation.[59, 70-72] Since both processes highly depend on pore size, the loading efficiency and release kinetics are directly correlated to particle porosity, requiring precise control and reproducibility of the process.[73] The surface of pSiO and pSi particles can be modified in order to attach targeting and other molecules through relatively simple processes guided by silane chemistry [47, 74, 75].

Until recently pSi was used in the format of powdered materials obtained by ultrasonic fracture[76, 77] or ball-milling [78] of the electrochemical etched pSi films. The resulting particles were characterized by their irregular shape and polydispersed size even though different subsequent sorting strategies were applied. Recent studies show that pSi particles of submicron and micron size can be fabricated by methods used in electronic industry, namely, photolithography and electrochemical etching.[74, 79] With 100 mm p^{++} Si wafer, photolithography and etching through the silicon nitride layer creates patterns of trenches (Fig. 2). The shape of the trenches is created by wet and dry etching process and is dependent on the nucleation mechanism of Si. After the formation of the Si particles on the wafer, high current density is applied which releases the particles from the wafer and suspends in isopropanol.[79] Afterwards, drugs can be loaded within the pores by simple capillary action. In particular, these pSi particles can be used as a multistage drug delivery system, called a multistage vector (MSV). In a MSV using pSi particles, drugs and other therapeutics can be carried, protected, and released using different layers and features on the particles.[80-83] The control over pore size, volume, thickness, and reproducibility of pSi are achieved easily in electrochemical anodization by varying the current during etching. We have studied these particles intensively and have been able to tailor the particle size, the pore size, and the shape to biological properties required.[79, 84]

Other etching methods, such as stain, photochemical, hydrothermal and galvanic, can also produce pSi particles. The problem with these methods is the limited reproducibility and production of non-uniform pores.[73] Other top down techniques for pSi particles is through sonication or ball milling of pSi layers. These techniques, however, produces polydispersed fragments of random size and shape.[79]

Mesoporous pSi particles are comprised of highly-ordered, hexagonal pore structures with empty channels.[85] SiO materials are stable and resistant to heat, pH, mechanical stress, and hydrolysis-induced degradation. As for pSi particles, the high surface area and tunable pore sizes allow for the adjustment of loading different drug concentrations and molecules into pSiO particles.[61]

Co-condensation, grafting, and imprint coating methods are the approaches to modifying mesoporous pSi particles.[61] As an example, Nakamura *et al.* successfully synthesized highly monodispersed thiol-functionalized nanoporous pSiO spheres with diameters in the submicron range using a surfactant-directed co-condensation of tetramethylorthosilicate (TMOS) and 3-mercaptopropyltrimethoxysilane (MPTMS) in a very dilute alkaline methanol–water mixture. In this study, the uniform spherical shape and the ordered hexagonal porous structure were simultaneously achieved at the molar ratio of MPTMS in the SiO source below 0.5.

2.5.Surface modifications

The surfaces of Si particles are typically covered by other atoms and substituents, including the hydrides, Si-H, Si-H_2, and Si-H_3. The Si-H, or silane, bonds are more reactive than C-H bonds due to the larger polarization and the relatively weak bond energy (318 kJ mol^{-1}) compared to hydrocarbon bond energy (411 kJ mol^{-1}). Silane bonds are stable only for short periods in air.[28] In addition, silanes readily oxidize in aqueous media. For biomedical applications, particle surfaces must be non-reactive when exposed to physiological temperatures, molecules, and environment. Passivating Si particles protects the surface from being reactive.[86] Surface treatments to stabilize the particles involve partial oxidation, stabilization with Si-C bonds, and bioconjugation. Partial oxidation is performed at 300°C, in which oxygen atoms attach to back-bonds of surface Si atoms instead of replacing hydrogen atoms. Partial oxidation changes the surface from hydrophobic to hydrophilic, an important feature for a drug delivery vehicle as it will be soluble in biological fluids.[86] Thermal, anodic, photo and chemical are also other techniques for oxidation.[87-90] Si-C is another method to make hydrophilic surfaces on Si nanostructures.[91-93] Using the hydrosilylation of alkenes and alkynes, the Si-C bonds replace the surface silane bonds. Thermal carbonization is another technique, in which the carbonized surfaces are stable in chemically harsh environments.[94] The silanol group used to synthesize SiO nanomaterial reacts with various compounds to form amine, carboxyl, and thiol groups. The versatility of SiO chemistry allows for an unlimited possibility of surface modifications using different biomolecules. SiO surfaces exhibit a negative charge. Oxidation of the Si surface generates hydroxyl units imparting the negative zeta potential to the Si particles (similarly to SiO surface), while conjugation of amino silanes (e.g. 3-Aminopropyltriethoxysilane (APTES)) inverts the zeta potential to positive. Both states can be used for subsequent functionalization of pSi with surface moieties. One technique, called the layer-by-layer (LBL) procedure, can effectively cover SiO NPs with controllable thickness by alternative layering of positive and negative charged polyelectrolytes on the surface.[98] Thiol chemistry on SiO NPs was demonstrated for the immobilization of oligonucleotides.[95] The conjugation of enzymes and antibodies to SiO surfaces were demonstrated using amine chemistry.[96] In addition, physical absorption of biomolecules, such as avidin[97], on SiO surfaces can also be used for passivation, but the weak interaction between the biomolecules and surfaces can be interrupted in a biological environment. Electrostatic interactions can also be used for SiO surface coverage.

The surface of the pSi and pSiO provides a suitable platform for the covalent conjugation and electrostatic attachment of a vast spectrum of targeting ligands, dyes, fluorophores, fluorescent tags, radioactive molecules and other functional moieties[65, 99-102]. Systems, such as phage displaying targeting peptides-gold nanoparticles networks (nanoshuttles[103])

can be easily attached to the surface of Si and SiO particles based on electrostatic interactions producing multifunctional nanoassemblies.[104] Well characterized silane chemistry enables the use of several commercially available bioconjugation kits to easily covalently functionalize the surface of Si and SiO particulates. This provides an opportunity for an incorporation of an imaging component, such as near infrared (NIR) dye, single photon emission computed tomography and positron emission tomography agents, while still keeping the pores available for loading drug agents overall creating a theranostic systems with synergistic functionalities[74]. As an example, in our recent study following conjugation of NIR probe to the surface of pSi hemispherical particles, the biodistribution in healthy mice was successfully tracked and the accumulation of the NIR-labeled pSi particles in the different organs was quantified based on image analysis[102].

In addition to the amorphous, crystalline and pSiO and pSi particles discussed above, many groups have developed other silicon based, nanosized structures, including nanowires, nanotubes, and nanocages. While their fabrication methods, stability and biocompatibility are not discussed here in detail, it is important to be aware that all these different structures are promising candidates as a drug delivery vehicle. The next few sections of this review describe the biocompatibility assessments of different silicon based nano- and micro-structures to four main routes of drug delivery (intravenous, inhalation, dermal, and oral).

3. Biocompatibility assessment for Si and SiO particles

Human exposure to Si based particles is increasing due to their high abundance in everyday (e.g. consumer) products as well as an increased interest in exploring the usage of Si and SiO particles as drug delivery carriers to tumors and other conditions. However, the adverse effects, induced by particles are not fully understood and are under extensive characterization. The four main external contact and drug delivery routes that we will cover in the following subsections are the intravenous injection, pulmonary inhalation, skin contact and gastrointestinal route (Fig. 1).

3.1.Effects of Intravenously administered Si and SiO particles

In intravenous injections, micro and nano-particles face multiple biological elements and boundaries as they travel to the targeted tissue. The main cell populations that come into the close and immediate contact with intravenously administered particulates are blood-born cells, such as erythrocytes, white blood cells (e.g. monocytes, neutrophils), tissue macrophages and endothelial cells aligning the vessel walls. Generally, if the endothelial wall is bypassed, the particles will be able to translocate to the epithelial cells. Macrophages recognize particles as foreign agents and aid to clear them out from the body. Below *in vitro* and *in vivo* studies about the contact of Si and SiO particles with body organs are being summarized, while *in vitro* interactions are divided to (1) cells involved in the vascular path, (2) macrophages, and (3) epithelial/stroma cells from cancer and other tissues.

3.1.1. *In vitro* studies with endothelial cells, blood-born cells and macrophages—In intravenous injections, Si based particles first encounter the blood environment and the vascular barrier of endothelial cells. Table 2, 3 and 4 summarize studies assessing Si- and SiO particles contact with endothelial cells, erythrocytes and macrophages, respectfully. A number of *in vitro* studies have reported that for amorphous SiO NPs the decrease in cell viability was dose and size dependent. Our works show that for pSi microparticles of different shapes and surface modifications, generally very low toxicity was observed following the contact with endothelial (Human Umbilical Cord Vascular Endothelial Cells, HUVEC and Human Micro-Vasculature Endothelial Cells, HMVEC) cells[65, 74, 102, 105-108]. As an example, we observed that following internalization of pSi microparticles, endothelial cells maintain cellular integrity, as demonstrated by cellular

morphology, viability and intact mitotic trafficking (Fig. 3)[106]. Moreover, as shown in Fig. 3, the presence of gold or iron oxide nanoparticles within the porous matrix did not alter the cellular uptake of particles, the viability of endothelial cells or rate of mitotic divisions. Endothelial cells maintained basal levels of proinflammatory cytokines IL-6 and IL-8 release in the presence of pSi particles. Interestingly, polarized, ordered mitotic sorting of endosomes bearing pSi particles within the daughter cells was observed.

An interesting recent work has compared the effect of nonporous SiO nanospheres produced by Stöber method, mesoporous Si nanospheres, mesoporous Si nanorods with aspect ratios of 2, 4, and 8 (Fig. 4), and their cationic charged counterparts on macrophages, erythrocytes and cancer epithelial cells. The authors observed cell-type-dependent toxicities of various particles. In general, cancer epithelial cells were not affected by SiO nanoparticles treatment, while macrophages responded differently to systems possessing various charges. Geometry did not have an effect on toxic reactions produced by the particles, while porosity and zeta potential prominently influenced cellular association of the particles and viability (Fig. 5) [109]. This difference in toxicity may result from intrinsic biological functions of the cells: while macrophages are professional phagocytes, being the first cells in the line of defense of the immune system, epithelial cells to not readily uptake foreign objects. As a part of the reticulo-endothelial system (RES), macrophages aid in the uptake foreign particulates introduced to the body. Thus, understanding the effects of nano- and micro- particles on macrophages is very important to estimate the overall toxicity. When particles are administered intravenously, adsorption of serum proteins (or opsonization) on the surface of the particles makes them more susceptible to contact with macrophages mediated by cell surface receptors. While particle uptake by macrophages can be used as a targeting strategy to inflamed regions, non-specific internalization by Kupffer cells (tissue macrophages of the liver) can cause a significant drop in the concentration of the particles in the blood.[110] Table 4 summarizes several *in vitro* studies on interactions of Si and SiO based particles with macrophages. In general, Si NPs induced more toxicity to macrophages at lower concentrations than Si microparticles. The high surface area in NPs may have an effect on decreased cell viability. It was also suggested that smaller particles may stimulate greater cytokine production than larger particles, explaining the higher toxicity at lower concentrations.[111]

In studies on erythrocytes, unmodified pSiO particles exhibited a porosity- and geometry-dependent hemolytic activity while pSiO particles with high aspect ratio caused significantly less hemolysis. It can be explained by the reduced contact area of porous particles with red blood cells membrane and by the fact that unlike their solid analogues, porous particles degrade to harmless orthosilicic acid[65, 105, 112]. Other studies confirmed that mesoporous pSiO and pSi particles demonstrate lower hemolytic activity than their nonporous analog, indicating the suitability for systemic drug delivery through the blood. [85] Our results of incubation of the pSi multistage carrier with whole mouse blood showed that the particles did not induce erythrocyte lysis and plasma contents of iron was not significantly different from untreated control. In contrast, incubation of the whole blood with positive control particles having sharp edges resulted in a significant increase of the iron contents in the plasma (12 μg/ml) indicating hemolysis of RBC [100].

3.1.2. *In vitro* studies with epithelial cells, fibroblasts and other cells—Studies summarized in Tables 5 and 6 present *in vitro* studies on contact of Si and SiO particles with epithelial, neuronal, stem cells, lymphocyte, and fibroblast cell lines. It is evident that particles cause a dose-dependent and time-dependent cytotoxicity on the cells. Moreover, the toxicity studied in *in vitro* tests depends on the cell type, particle size, particle shape, particle structure, and aggregation state. Yuan *et al.* demonstrated that the size of the NPs is a critical parameter to induce toxicity. After exposing human embryonic kidney cells

(HEK293) to various sized SiO particles at dosages ranging from 20 to 2000 μg/ml for 24 hours, smaller (20 nm) SiO particles exhibited more cytotoxicity than the larger SiO particles (50, 80, 140, 280, and 760 nm). Cells also presented with apoptosis after incubation with 20 nm SiO particles.[122] Furthermore, most of the *in vitro* studies presented used the MTT (3-(4,5-Dimethylthiazol-2-yl)-2,5-diphenyltetrazolium bromide) test to measure the cell viability. Fisichella *et al.*, however, investigated that Si based particles can promote exocytosis of the formazan crystals from the MTT assay and can falsely estimate the cell viability.[123] In addition, *in vitro* assays usually provide short-term effects on the cells.

The next section focuses on *in vivo* studies evaluating effects of intravenously administered Si and SiO particles.

3.1.3. *In vivo* studies on intravenously administered Si and SiO particles—It is difficult to extrapolate the *in vitro* results to *in vivo* effects. *In vivo* studies provide more relevant information such as the effect of Si based particles on the system as a whole including effects on all the separate elements, as well as the long-term outcomes. Table 7 summarizes a number of *in vivo* studies with systemically injected Si and SiO particles. Several studies have shown that pSi and pSiO particles were cleared out within a month from the body with no system toxicity [14, 131]. An effective clearance can prevent toxicity induced by residual metal ions and foreign materials in the body. Most of the porous particles were deposited in the liver and spleen. In a study by Huang *et al.*, th dependence of clearance on the shape of the particles was observed. Short rod-shaped SiO NPs were trapped in liver and cleared out quickly, while long rod-shaped SiO NPs were trapped in the spleen.[14] Lu *et al.*, however, reported that although clearance of non-porous NPs was significantly delayed, there were no differences in cell metabolic profiles.[132] It is known that nonporous Si and SiO materials is not easily degradable, which can explain this observation. Still, nonporous amorphous Si based particles displayed no significant toxicity to mice. Following acute (single injection) and sub-chronic (four consecutive injections with 1-week difference in between) injections, biocompatibility of negatively (−33mV) and positively (+9mV) charged pSi microparticles was examined[133]. No change in plasma levels of renal (BUN and creatinine) and hepatic (Lactate Dehydrogenase, LDH) biomarkers as well as 23 plasma cytokines was observed as compared to saline injected animals (negative control). pSi microparticles also did not alter LDH levels in liver and spleen, nor lead to infiltration of white blood cells into the major organs, suggesting that they are safe to be used as a carrier for drug delivery. Overall the *in vivo* studies on the cytotoxicity of Si based particles displayed no immunogenic and toxicity issues.

Another interesting biocompatibility issue with the delivery of nano and micro particles as drug delivery vehicles is their possible application in pregnancy. We were first to report that there is a particle size dependency on the translocation through the placenta.[140] The 834 nm and 1 μm Si particles were not able to pass through the placenta in pregnant rats, whereas, the 519 nm Si particles were found in the fetus (Fig. 5). In the following study, by Yamashita et al., smaller sized SiO particles (70 nm) were found in the fetal liver, fetal brain, and induced complications at high concentration of 0.8 mg per mouse.[141] It was concluded that SiO delivery to pregnant rats can be detrimental to the fetal development. The fetus is extremely sensitive to the environment and therefore, the addition of small sized particles can cause adverse effects.

3.2. Si and SiO particles administered through Inhalation

Pulmonary route represents another drug delivery approach. Additionally, lungs represent one of the most frequently contacted organs by air-born particles. Brownian diffusion allows particulates to travel in air, creating a possibility of inhaling drug-loaded particles.[16]

Particles can easily reach the lungs, travelling through the nose and larynx.[142] For diseases, such as lung cancer, designed particles can target lungs in order to treat and image the tumor site. Si-based nanomaterials, however, has not exhibited promising results. As an example, exposure to crystalline SiO has resulted in various respiratory diseases, such as silicosis, interstitial fibrosis, industrial bronchitis, small airway disease, and emphysema. [143-146] In contrast, amorphous SiO is considered to be less toxic for inhalation applications. The *in vitro* and *in vivo* studies on Si-based materials contact with lung cells/ tissues are summarized in Tables 8 and 9, respectively.

Most of the *in vitro* studies with A549 epithelial human lung cells[148] reported a time and dose-dependent decrease in proliferation induced by Si based particles, regardless of the size in the sub-micron range. Furthermore, Ale-Agha *et al.* reported that the gap junctional intercellular connection (GJIC) is an important factor in *in vitro* toxicity. After the treatment with ultrafine SiO NPs, GJIC decreased by 77%, indicating the reduction in intercellular communication and signaling.[147]

Controversial *in vivo* data about pulmonary exposure to Si and SiO particulates can be found in the literature. The comparison between the results obtained in various studies is not trivial due to the use of different dosages, time points, and animal models. Interestingly, in one study SiO nanorods administered into mice demonstrated no toxicity compared to control tissues between a 5 – 14 hours exposure.[154] This indicates that shape plays a significant role in interaction of Si-based materials with lung tissue and this factor should be considered when designing nanostructures for drug delivery applications through inhalation.

Chen *et al.*[142] studied whether the age of the animals should be a concern when understanding pulmonary toxicity of air-born particles. The factors that vary with age of the animals are: lung volumes, respiration rates and metabolism. Since old rats have a higher respiration volume, higher uptake of SiO NPs is expected when compared to younger rats. This could be a reason for observing a massive infiltration of inflammatory cells in the old rats and no significant levels of the above in younger rats.[142]

While these studies attempt to understand the potential pulmonary toxicity induced by Si based particles using *in vitro* and *in vivo* models, it is important to realize that clinical evidence on the exposure to SiO NPs has been reported. Song *et al.* studied a group of patients that were exposed to NP-filled aerosol paint. Patients exhibited mysterious symptoms of pleural effusions, progressive pulmonary fibrosis, and pleural damage. Within three months of the onset of illness, 20 nm SiO NPs were found in pulmonary microvessels, vascular endothelial cells, macrophages and microlymphatic vessels. After eighteen months of the disease, the amount of nanoparticles found in the pulmonary cells and macrophages was lower, but fibrous SiO nanostructures with lengths around 70 nm were detected in the nucleus and cytoplasm of alveolar epithelial cells.[158] It is thought that the exposure to SiO NPs from aerosol paint may have contributed to the patients' illnesses. Therefore, it is important to completely understand the issues underlying nanosystems prior to using them.

3.3. Skin contact of SiO particles

Dermal exposure is one of the most common ways of contact with air-born particulates. NPs in air can contact skin surface and in some (rare) cases permeate the skin barrier. Moreover, dermally applied drugs constitute one of the largest branches of pharmaceutical market. High concentrations of a therapeutic agent can be applied at the topical site targeting a pathological condition and reducing systemic side effects.[159] The skin is the organ with the largest surface area that is in contact with particulates distributed in the air. Its intrinsic property as a permeability barrier, however, prevents the vast majority of nanoparticles to cross it and to be absorbed systemically by viable tissues. [99, 160-162]

Understanding the structure of the skin barrier is imperative for an evaluation of the possible fate of particles contacting the intact skin. The skin is a multilayered organ with the main two compartments being epidermis and dermis (Fig. 6). Epidermis, and particularly its outermost layer, stratum corneum (SC), represents the most important control element in transport of substances into and across the skin. SC can be described as a "brick and mortar" structure where the bricks are corneocytes, terminally differentiated metabolically inactive cells of the skin epithelia filled with insoluble keratins, and mortar is the continuous intercellular lipid phase, composed mostly of ceramides, cholesterol, free fatty acids and cholesteryl esters[163]. This unique chemical composition of SC and very low water content (~15% w/w) impart to this protective layer a highly lipophilic nature. Thus, only low molecular weight xenobiotics (<500 Da) with intermediate lipophilicity or specially designed carriers can cross this intrinsic barrier and be absorbed to the deeper layers of the skin or, through the network of blood capillaries located in the dermis, to the systemic circulation.[163] Generally, a substance applied on the skin surface has three possible ***routes*** to reach the viable tissue: *intercellular* through SC lipids, *transcellular* across the corneocytes, and *transappandageal* via skin appendages (hair follicles, eccrine sweat ducts, etc.) (Fig. 6). The majority of free molecules are believed to be absorbed through the intact SC through the intercellular tortuous route. Because of the low fractional appendageal area (about 0.1%), except for ions and highly polar molecules that struggle to cross intact SC, this pathway usually adds little to steady-state drug flux. However, appendages may function as shunts, which may be important at short times prior to steady-state diffusion. Additionally, particulates can specifically target this route.

Application of SiO particulates on the skin surface is generally considered safe. It is noteworthy that sol-gel systems, introduced by Avnir in 1984, were approved for treatment of rosacea and acne and have been used in sunscreen formulations. Still, as for any other systems, controversial results regarding their interactions with skin can be found in the literature. There are no systematic studies on the contact of Si particles with the skin. Table 10 summarizes a number of studies about the interaction of SiO particles performed on *in vitro*, *ex vivo*, and *in vivo* skin models. In an *in vitro* study with human keratinocytes (HaCaT), Park *et al.* observed dose-dependent cell viability after the treatment with 7 nm and 10 nm SiO particles.[164] Zhang *et al.* observed that size-dependent cytotoxicity using SiO NP (80 and 500 nm).[165] Compared to the 500 nm SiO NPs, the 80 nm SiO NPs decreased cell viability and blocked cell proliferation for human dermal fibroblasts. As mentioned previously, this result may be due to the large ratio of surface area to weight in smaller NPs, causing more side effects. The 80 nm SiO particles induced a disruption of the mitochondria membrane, which may have resulted in mitochondria dysfunction and cytotoxicity. In the scratch test, the addition of SiO particles decreased the rate of healing. [165] Nabeshi *et al.*[166] have evaluated size-dependent intracellular localization and cytotoxicity of SiO particles, using the mouse epidermal Langerhans cell line, XS52. Langerhans cells are the skin macrophages located in the viable epidermis. The results suggest that 70 nm particles had significantly higher uptake and cytotoxicity than 300 and 1000 nm particles. Although these studies were performed in 2D culture, they provide preliminary information on the effects of cellular function with the addition of SiO particles to skin cells. However, it should be kept in mind that in order to reach viable strata of the skin, the particles should first bypass the metabolically inactive skin barrier.

As the skin possess many layers of different types of cells, it is useful to test cytotoxicity and obtain relevant results on three-dimensional (3D) *in vitro* cultures, *ex vivo* tissues, and *in vivo* systems. EpiDerm™ skin model is a 3D culture model of human keratinocytes that includes a cornified layer that mimics the skin morphology. No significant change in cell viability was observed in this model after treatment of SiO NPs (7 and 10 nm) at high concentrations of 500 μg/ml for 5 hours and 18 hours.[164] Additionally, *ex vivo* models

are valuable in understanding the interactions of NPs to the different layers of the skin. Graf *et al.* have demonstrated that sub-micron particles in buffered solution were distributed around the stratum corneum and in the hair follicles in an *ex vivo* model of plastic surgery patient skin samples.[169] In an *in vivo* study, SiO NPs (50 nm) aided submicron emulsions to penetrate into the epidermis and dermis of pigs after 6 hours exposure.[170] Additionally, the Draize skin test, an acute toxicity assay devised by the FDA, revealed no evidence of edema or erythema in rabbits after 24 or 72 hours of application of SiO particles.[164]

Skin penetration is highly dependent on the surface properties of the particle. While SiO NPs with surface hydroxyl group increase the hydrophilicity of the drug delivery systems and is able to protect on the active payload[159], a critical parameter to consider is the isoelectric point.[168] The isoelectric point for SiO is 2.3 to 2.8[171] and for skin is 3.5 to 4.8, making both surfaces negatively charged under physiological conditions.[159] By modifying the surface of the particles to positive charge, SiO particles can be attracted to the negatively charged skin surface.

Sunburn and some types of cancer are related to UVB (280 – 315 nm) radiation as DNA is damaged by the formation of thymine-thymine dimers. Sun-tanning, photoaging, and malignant melanoma are due to UVA rays (315 – 400 nm) that damage DNA by free radical generation. According to the material properties and simulations, Popov *et al.* reported that Si particles effectively attenuate the 400 nm signal compared to titanium oxide particles, suggesting that Si particles can aid in prevention of UVA radiation.[172]

In general, solid particles of >20nm in diameter are not expected to penetrate the intact SC layer, although they may accumulate in skin shunts. Thus, products based on SiO particles are being approved for the treatment of conditions involving skin appendages, such acne and rosacea.

3.4. Contact of Si and SiO particles with gastrointestinal tissues

Gastrointestinal (GI) route represents the most common and patient-compliant way of drug administration. However, some of the drugs have poor pharmacokinetic profiles when administered orally.[118] The major barriers in oral delivery are the enzymes in the upper parts of the GI system, the pH changes in the GI tract, absorption and efficient permeability across the intestinal wall[173], presence of bile salts[60] and liver-mediated first pass metabolism.[118] The pH levels change throughout the GI tract, the pH in the stomach is 1 – 3 while in the small intestine, the pH is 6.5 – 7.0 and in the colon, it is 7.0 – 8.0.[174] Drug absorption occurs through paracellular transport along the epithelial lumen of the small intestine. However, the tight junctions among adjacent enterocytes form a barrier for drugs. [175] The presence of bile salts can affect the structure of the drug molecule and therefore, its function. The absorbed drugs then pass through the entero-hepatic circulation, and the “first-pass metabolism” in liver can clear the active agent before reaching the systemic circulation and the intended site.

In this type of complicated environment, Si and SiO particulates can have clear advantages for overcoming various hurdles of oral delivery and protecting the encapsulated molecule. Si and SiO-based materials are hydrophilic which increase the wettability of water-insoluble drugs in the GI tract.[176] Moreover, since Si and SiO particles are low-pH resistant there is a clear the rationale for using them as a drug delivery system for orally administered drugs to protect from low pH in stomach.

In one *in vitro* study, the toxicity induced in human esophageal epithelial cells (NE083) was studied with crystalline and amorphous SiO NPs. The crystalline SiO NPs showed a dose-dependency on Caco-2 cell viability. Compared to crystalline SiO, amorphous SiO NPs

were less toxic at doses ranging from 0.156 to 10 μg/ml. TEM analyses has shown that the morphology of esophageal epithelial cells did not change following uptake of amorphous SiO NPs. For crystalline SiO NPs, however, it was observed that the organelle membrane ruptured and there was direct contact between the NP and cytoplasm, which may lead to direct chemical exchange and toxicity in esophageal epithelial cells.[177]

Under *in vivo* conditions, SiO NPs (diameters of 70, 300 and 1000 nm) were administered to mice at a maximum dose of 100 mg/kg. The 70 nm SiO NPs were lethal to mice at doses greater than 20 mg/kg, while the 300 and 1000 nm SiO NPs did not affect the mice. Also, no toxicity and abnormalities were observed in any of the analyzed organs (spleen, kidney, and lung) after the administration of the 300 and 1000 nm SiO NPs. However, after the administration of 70 nm SiO NPs, degenerative necrosis of hepatocytes in the liver was observed and after chronic administration of 70 nm SiO NPs, liver fibrosis was observed. [178] These *in vivo* studies reiterate that potential toxicity through oral delivery is highly dependent on the size of the NP carrier. As mentioned above for studies involving erythrocytes and skin, surface area of small sized particles plays a major role in cytotoxicity during GI exposure. For large sized particles, however, the size properties may be more dominant than surface area properties, which may have reduced toxicity.

In addition to non-porous SiO NPs, pSi and pSiO are being investigated as oral drug carriers, due to their large pore volumes and thus the ability to load drugs in the pores. Possessing a high surface free energy due to their large surface area, drug molecules can be absorbed into the pores to reach a low state of free energy. Orally-administered drugs can be loaded and protected in pSi based particles due to the large surface area, large pore volume, highly ordered pore structure, and adjustable pore size. The large surface area and pore volume of mesoporous pSi and pSiO particles allow drug molecules, that are water insoluble, to remain dispersed within the pores and improve absorption.[179] Oral absorption of molecules/drugs, such as naphthalene[60], itraconazole [180, 181], antipyrine[78], ibuprofen [78, 182, 183], griseofulvin[78], ranitidine[78], furosemide[78], indomethacin [179], insulin [175], telmisartan [184], and sulfasalazine [185], loaded into mesoporous pSi and pSiO particles have been reported. While these studies demonstrate promising results for mesoporous pSi and pSiO particles as oral drug delivery carriers, there are still only a few studies characterizing their safety profile in the GI tract.

The stability of pSi particles is important in the GI tract. It was shown that bare pSi exhibited high surface oxidation after eighteen hours incubation in simulated intestinal fluid. [186] After functionalization with alkyl groups, Albrecht *et al.* demonstrated that the porous particles had high resistance to oxidation in the gastric and intestinal fluids.[186] Surface oxidation and other chemical/physical exchanges between the particle and GI environment can produce unpredictable toxicity by reactive oxygen species (ROS). However, if the particles are already oxidized, the contribution of these processes can become negligible.

Consistent with the idea that toxicity is dependent on surface area, Bimbo *et al.* observed that pSi microparticles (10 – 25 μm) induced more toxicity by decreasing cell viability than small porous silicon particles (97, 126, 164 nm) in human colon carcinoma cells (CaCo-2). Unlike nonporous SiO particles, pSiO exhibit large surface areas, which may be causing toxicity in cells. In non-toxic concentrations, microparticles were not internalized by the CaCo-2 monolayers but were in close proximity to cells.[118] At higher concentrations (2 – 14 mg/ml) of mesoporous pSiO microparticles, Caco-2 cell membrane integrity weakened along with diminished cell metabolism and increased apoptotic signaling.[183] Smaller porous particles (50 nm) also exhibited insignificant toxicity after treating at various concentrations from 1 to 500 μg/ml in human colon cancer cell line (HT-29).[174] It was observed that cell viability was particle size dependent, while the production of intracellular

ROS was particle concentration dependent. Although the 1- 10 μm particles produced a high level of ROS in CaCo-2 cells, it was significantly lower than ROS production from the administration of H_2O_2 (positive control). In addition to inducing low toxicity, these particles degraded over time, allowing for the potential controlled release of drugs. In *in vivo* experiments, there was no evidence of toxicity in rabbits and dogs that were administered with mesoporous silica particles (0.2 – 1 μm) orally.[180]

Other types of oral delivery carriers using Si and SiO materials have also been investigated. Tan *et al.* developed a SiO-lipid hybrid microcapsule that enhanced drug dissolution characteristics and improved absorption.[176, 187] Si-nanowires coated with SiO microparticles enhanced particle adhesion and drug permeability.[188] However, the effects induced in the GI tract for these unique structures have not been investigated.

In general, more careful and systematic studies on the effects of Si and SiO particles in the GI tract are highly demanded. It is especially true, due to the fact that high drug/delivery system doses (> 200 mg) are required for oral administration. *In vitro* studies, therefore, do not provide the entire picture as most *in vitro* studies test the effects of lower concentrations. [183] Moreover, oral toxicity was primarily assessed by the data from the MTT assay. The colorimetric test on *in vitro* cultures, however, should not be final judgment on cytotoxicity issues since it was reported that MTT test results can be impaired by pSi particles with oxidative potential [189]. The toxicity observed is not necessarily from the immediate processes that directly affect cell viability, rather it may arise from the alterations on the genetic level.

4. Genotoxicity of SiO particles

Introducing NPs into cells can cause adverse effects at a genetic level, which is called genotoxicity. Cytotoxicity is when cell death (necrosis) occur from membrane lipid peroxidation, membrane rapture, energy depletion, or organelle destruction, whereas, genotoxicity is when cell death is due to apoptosis and changes in interconnected signaling pathways.[190] The biological structure of DNA is designed to store information with great stability, thus any type of mutation and damage to DNA molecules can affect cellular processes and functions. Moreover, genetic instability is largely associated with different forms of cancer. Therefore, it is important to understand the potential genotoxicity induced by particles that are delivered as drug vehicles and are internalized by cells.[191]

Particulates can affect the genes either directly or indirectly, which is termed as primary or secondary damage (Fig. 7). The main mechanism to induce genotoxicity is the ability of particles to produce oxidative stress.[191] Oxidative stress is the imbalance between ROS and antioxidant conditions in the cell. ROS is responsible for oxidation of DNA bases, breakage of DNA strands, and lipid peroxidation-mediated DNA adducts.[192] In the primary mechanism, metal NPs, depending on their physical and chemical properties, can directly produce oxidants, such as highly reactive hydroxyl radicals (OH•). Insolubility and surface properties of NPs are main factors to directly affect cell genotoxicity. Although not common, small NPs can directly affect DNA by permeating into the cell nucleus. As an example, small SiO NPs (40 – 70 nm) were found in the nucleus of HEp-2 cell (human epithelial) directly contacting DNA strands during mitosis.[193] Also, free metal ions from particles can induce permeability of nucleus barriers, therefore, indirectly damaging DNA molecules. Additionally, particles can stimulate mitochondria in cells to produce ROS which can destabilize genetic material of the cells. In the secondary mechanism, genotoxicity arises from inflammation. Particles can induce inflammatory cells, such as macrophages, to produce and deliver oxidants to cells. [191, 192] The efficiency of intra- and extracellular

defense systems for antioxidants and repair systems for DNA is important in determining the secondary genotoxicity.[192]

Genotoxicity can be tested using different approaches. The genotoxic potential of particles can be evaluated by using non-cellular, biochemical techniques that examine the conformational changes and strand breakage of DNA, by *in vitro* assays that mainly test for primary mechanisms, and by *in vivo* assays that test both primary and secondary genotoxic mechanisms.[192] The comet assay is the standard test performed to examine potential genotoxicity induced in cells. It is used to examine bacterial reverse mutations and the *in vitro* mammalian chromosomal structural aberrations. It is used to analyze the unrepaired DNA strands and alkali-labile DNA base sites in cells. At a higher pH (> 13), the assay is able to detect DNA lesions and single-strand breaks with higher sensitivity, which is called the alkaline comet assay.[191] Using basic electrophoresis concepts, the assay can provide different parameters, such as tail length, percentage DNA in the tail, and tail moment, indicating the amount of DNA breakage.

In 1997, crystalline SiO was classified as a carcinogen by the International Agency for Research on Cancer.[194] However, an independent review by Borm *et al.* stated that *in vitro* and *in vivo* studies performed after 1997 show evidence that the crystalline SiO particles was not completely carcinogenic, but rather induced genotoxicity by the secondary mechanism, stimulating inflammation.[195] Amorphous SiO particles, however, were found to be safe.[191] Jin *et al.* tested negative in the alkaline comet assay on human lung epithelial cells (A549) when using 50 nm SiO NPs doped with luminescent dyes.[190] In the lungs, it was reported that glutathione (GSH), an antioxidant found in lungs, protected against possible cell injury and genotoxicity induced by 5 μm crystalline SiO particles in rat alveolar macrophages.[196] Likewise, Wang *et al.* tested amorphous SiO particles of 7 nm in size on WIL2-NS, a human B-cell lymphoblastoid cell line, and reported a negative result in the alkaline comet assay. The authors, however, reported positive results after the hypoxanthine guanine phosphoribosyltransfease (HPRT) gene mutation test. [197] In another study, after treatment with 14 nm SiO NPs, no increase in DNA damage was detected, but the number of oxidatively produced lesions slightly increased in Caco-2 cells. [198]

Choi *et al.* reported that SiO NPs (10 nm) may cause primary DNA damage but not mutagenicity in both the mouse lymphoma (L5178Y) and human bronchial epithelial cells (BEAS-2B).[199] Additionally, hypomethylation of DNA was found after the treatment of human keratinocytes (HaCaT) with SiO NPs.[200] Jin *et al.* observed that luminescent SiO NPs induced an increase in hOgg1 enzyme (related to DNA repair) expression, but no change in enzyme activity in A549 cells.[190] After the exposure to SiO particles (14 nm), Ale-Agha *et al.* observed changes in the subcellular localization of connexin-43 and of β-catenin, proteins for gap junctional intercellular communication, in rat lung epithelial cells (RLE).[147] Interestingly, Huang *et al.* reported that mesoporous SiO NPs decreased ROS production in human malignant melanoma cells (A375), a skin cancer cell line, but adversely caused an increase in cancer cell proliferation.[201] While these few described studies exhibit minor evidence of genotoxicity, it is still unknown whether the oxidative stress formed was through direct or indirect mechanisms.

One of the main reasons for oxidative stress is due to changes in particle surface properties. Barnes *et al.* found no genotoxicity SiO NPs (30, 80, and 400 nm) with different surface coatings (alumina coated (chloride-ion stabilized), sodium counter-ion stabilized, and unstabilized) at the dose of either 4 or 40 μg/ml in 3T3-L1 fibroblasts. [202] In addition, there was no evidence of oxidative stress due to particle aggregation. Similarly, Park *et al.* tested the size dependency (10, 30, 80, and 400 nm) on chromosomal aberrations using the

micronucleus assay and gene mutations using the *lacZ* gene mutation assay in 3T3-L1 mouse fibroblasts.[203] In these cells, 80 nm silica particles induced chromosomal aberrations, while both the 30 and 80 nm particles induced gene mutations. In addition, another study demonstrated that although the uptake of SiO particles (80 nm and 500 nm) in fibroblasts did lead to excess production of ROS, the particle internalization decreased the mRNA levels for fibronectin and laminin, which are related to the adhesion characteristic of the cells.[165] In another study, Waters *et al.* observed that genotoxicity was not induced by particle number or mass, rather it was induced by particle surface area.[120] While these studies do not indicate a direct dependence of size on genotoxicity, there is evidence that small sized NPs can cause genotoxicity compared to large sized NPs due to the high surface area.[204]

In addition, the type of cell that is being tested can also influence the genotoxic outcome. For example, cells with long doubling times were more susceptible to damage than cells with short doubling times, such as cancer cells.[202] In a recent study Yang *et al.* explored the interrelationship between particle size and shape by testing four types of particles with distinct chemistries, namely carbon black (CB), single wall carbon nanotube, SiO and zinc dioxide (ZnO) NPs. Following the examination of cytotoxicity, genotoxicity and oxidative effects of particles on primary mouse embryo fibroblast cells, it was found that ZnO induced the most cytotoxicity, and intracellular oxidative stress levels (measured by ROS generation, glutathione depletion and malondialdehyde production). In this work, SiO (~ 20 nm)were found to be safer than the comparative systems, showing the importance of particle composition in the cytotoxic effects of different NPs, while the potential genotoxicity might be mostly attributed to particle shape [205].

Similarly, different cell types *in vivo* demonstrated different genotoxicity levels when using Si NPs (2 – 5 nm). A study done on mice by Durnev *et al.* revealed evidence of DNA damage in bone marrow cells within 24 hours of exposure of small Si NPs at a dosage of 5 mg/kg.[206] Increasing the dosage to 50 mg/kg caused DNA damage to brain cells as well within 24 hours. Si-based particles have also been explored as a gene carrier, demonstrating promising results to effectively transfect and deliver genetic material.[207-209] Studies for Si NPs related effects on genetic toxicity should be carried out to understand possible risks.

It is difficult to compare and make a conclusion based on all the studies regarding the probable genotoxicity mechanisms for Si based particles. Each study used a different dosage in their tests, making it difficult to compare as genotoxicity is dosage dependent. Other factors can also affect the genotoxicity outcome, such as the number of internalized particles and the different types of cells used in the study. This, in turn, will produce different exposure mechanisms of particles to DNA during mitosis. In addition, it has been found that the level of serum can modulate the cellular response and therefore, minute details in each study can affect the overall outcome of genotoxicity induced by SiO and Si particles.

5. Conclusions and future outlook

In this review, we focused on Si based nano- and microparticles effects following various administration/exposure routes. Silicon is an element found in nature and humans have utilized Si based materials since ancient times. In general, the use of Si based materials is not considered harmful to humans. Due to the unique properties of silicon, Si based particles have become of great interest in many fields of science, including pharmaceutics. However, the short and long term effects of human exposure to Si and SiO particles are not completely understood. In general, crystalline SiO is considerably more toxic than amorphous SiO and Si particles. It was also shown that nanoparticles (<100 nm) induce more significant effects on cells and animals than larger particulates. Still, since not many systematic studies

evaluated the effect of size, geometry and surface properties on the toxicity levels in cells and tissues, it is hard to draw solid conclusions. It is known that particle size, surface, shape, and chemistry play a major role in determining the effects in cells, so it is reasonable to anticipate that these effects will be translated to toxicity levels. Moreover, in spite of keeping the particle's physical and chemical variables constant, different types of cells and tissues behave differently in the presence of particles due to their varying metabolic rates, permeability, and functions, making the issue of categorizing Si based particles based on biocompatibility very difficult.

As it can be inferred in this review, the studies lack standardization for comparison. It could be of a great value to have a set of positive and negative controls that can be used across different laboratories to understand the inter-person and inter-laboratory variations in the obtained data. In addition to these factors, it is also important for laboratories to use the same terminology and definitions in their studies. There have been great efforts from national institutions, such as National Institute of Standards, and Technology (NIST) and National Cancer Institute (NCI), to find an approach to standardize the methodology for determining nanoscaled toxicity and aid in clinical translation of particles.[16] It was also suggested that standardization can be achieved by using common experimental set up (same cell line and animal model), and exposure conditions (cell confluency and exposure duration).[7]

One major parameter that is making toxicology studies of particles difficult to compare is the use of concentrations to determine the dosage of particles. The units for concentrations were made useful when describing a drug or an agent as one molecule. Therefore, in the simplest form, concentration is used to explain the number of molecules (by mass) in a given volume of solvent. This normalized unit, however, does not completely describe the number of particles administered in a human body. A particle is made up of several molecules, creating a physical structure of a specific size, shape, and surface. In many of the studies described in this review, smaller sized particles induced more toxic effects on various cells than larger sized particles. It was concluded, however, that it is not the size, but the surface area, of particles that can cause different toxic effects. In addition to surface area, the number of particles internalized into the cells also affects the level of toxicity. The terminology for dosimetry of NPs may aid to improve the normalization of administered particles to cells. One approach is to report the number of particles rather than the concentration of the elemental mass.[22, 155] Using the particle number, however, may not be the exact number of particles internalized in cells, as each type of cell has different endocytosis mechanisms.[16] Additional approach that can be taken is to define surface area. This metric of dosage may be more accurate as it normalizes to size and shape of the particle. Yet, a study performed by Lison *et al.* demonstrated that total particle mass or concentration provides similar results in different cell lines with different cell assays, concluding that for *in vitro* tests on SiO NPs, concentration is sufficient.[150]

Another factor that affects obtaining relevant toxicology information of particles is the use of *in vitro* and *in vivo* studies. Two-dimensional *in vitro* models are necessary to understand the initial response to a particular cell line. The cell studies, however, do not provide the complete story on how the body reacts to particulate objects, as many responses are related to 3D architecture of the tissue and the microenvironment in the particular organ (e.g. presence of macrophages and other inflammatory cells). Consequently, *in vivo* studies (with the use of the correct animal models) are extremely advantageous as researchers can obtain extensive information on the short term immune responses as well as long term toxicity issues. Obtaining reproducible results from animal models, however, is expensive. Therefore, it may be more useful for laboratories to use three dimensional (3D) *in vitro* models that are cost effective while mimicking the human biological responses. In 2D *in*

vitro tests, cells are attached to plastic/glass surfaces that affect their behavior compared to their native state which is in 3D tissue form (attached to each other and other cell types. Forming a 3D co-culture of different cell lines in a gel matrix or solution can better represent the tissues' structure and function *in vivo* and provide more relevant information on cellular/tissue response to particles. Several groups have studied the influence of NPs on 3D *in vitro* models [210-212], but it is not as popular as using the conventional 2D *in vitro* tests.

The pharmaceutical industry is keen on utilizing nanostructures as drug delivery vehicles. There are a number of evidences in the clinic that demonstrate the incorporation of therapeutics and drugs within particles enhances drug efficacy and improves treatment of conditions through various administration routes. As a result, possible adverse effects induced are a major concern. The research community and drug developers would greatly benefit if experimental standardizations are set for NP studies in biological applications.

Acknowledgments

We would like to thank Srimeenakshi Srinivasan and Fransisca Leonard for their informative discussions on the manuscript. We also would like to thank Matthew Landry for his assistance with graphics in the manuscript. The authors acknowledge a financial support from the following sources: Susan G. Komen Postdoctoral Fellowship #PDF12229449, NIH U54CA143837 (CTO, PS-OC), NIH 1U54CA151668-01 (TCCN, CCNE), DODW81XWH-09-1-0212 and DOD W81XWH-11-02-0168.

Abbreviations

APTES	3-Aminopropyltriethoxysilane
ELISA	Enzyme-linked Immunosorbent Assay
GI	Gastrointestinal
HMVEC	Human Micro-Vasculature Endothelial Cells
HUVEC	Human Umbilical Cord Vascular Endothelial Cells
ICP-AES	Inductively Coupled Plasma Atomic Emission Spectroscopy
ICP-OES	Inductively Coupled Plasma Atomic Emission Spectrometry
ICP-MS	Inductively Coupled Plasma Mass Spectrometry
LBL	Layer-by-layer
LDH	Lactate dehydrogenase assay
MSDS	Material Safety Data Sheet
MSV	Multistage Vector
MTS	Cell Viability assay using 3-(4,5-dimethylthiazol-2-yl)-5-(3-carboxymethoxyphenyl)-2-(4-sulfophenyl)-2H-tetrazolium
MTT	Cell Viability assay using 3-(4,5-Dimethylthiazol-2-yl)-2,5-diphenyltetrazolium bromide
NCI	National Cancer Institute
NIR	Near Infrared
NIST	National Institute of Standards and Technology
NP	Nanoparticles

pSi	Porous Silicon
pSiO	Porous Silica
RBC	Red Blood Cells
RES	Reticuloendothelial system
ROS	Reactive Oxygen Species
SC	Stratum Corneum
Si	Silicon
SiC	Silicon Carbide
SiO	Silica
WST-1 or WST-8	Cell Viability assay using 2-(4-Iodophenyl)-3-(4-nitrophenyl)-5-(2,4-disulfophenyl)-2H-tetrazolium, monosodium salt or 2-(2-methoxy-4-nitrophenyl)-3-(4-nitrophenyl)-5-(2,4-disulfophenyl)-2H-tetrazolium
XTT	Cell Viability assay using 2,3-bis-(2-methoxy-4-nitro-5-sulfophenyl)-2H-tetrazolium-5-carboxanilide

References

[1]. Ma JF. Plant Root Responses to Three Abundant Soil Minerals: Silicon, Aluminum and Iron. Critical Reviews in Plant Sciences. 2005; 24:267–281.

[2]. Daniel E M. Silicon biotechnology: harnessing biological silica production to construct new materials. Trends in Biotechnology. 1999; 17:230–232.

[3]. Kenneth KO, Kim K, Floyd BA, Mehta JL, Yoon H, Hung CM, Bravo D, Dickson TO, Guo XL, Li R, Trichy N, Caserta J, Bomstad WR, Branch J, Yang DJ, Bohorquez J, Seok E, Gao L, Sugavanam A, Lin JJ, Chen J, Brewer JE. On-chip antennas in silicon ICs and their application, IEEE Trans. Electron Devices. 2005; 52:1312–1323.

[4]. Van Dyck K, Van Cauwenbergh R, Robberecht H, Deelstra H. Bioavailability of silicon from food and food supplements, Fresenius. Journal of Analytical Chemistry. 1999; 363:541–544.

[5]. Braley S. The Chemistry and Properties of the Medical-Grade Silicones. Journal of Macromolecular Science: Part A - Chemistry. 1970; 4:529–544.

[6]. Luhrs AK, Geurtsen W. The application of silicon and silicates in dentistry: a review. Prog Mol Subcell Biol. 2009; 47:359–380. [PubMed: 19198786]

[7]. Lewinski N, Colvin V, Drezek R. Cytotoxicity of nanoparticles. Small. 2008; 4:26–49. [PubMed: 18165959]

[8]. Barbé C, Bartlett J, Kong L, Finnie K, Lin HQ, Larkin M, Calleja S, Bush A, Calleja G. Silica Particles: A Novel Drug-Delivery System. Advanced Materials. 2004; 16:1959–1966.

[9]. Auffan M, Rose J, Bottero J-Y, Lowry GV, Jolivet J-P, Wiesner MR. Towards a definition of inorganic nanoparticles from an environmental, health and safety perspective. Nat Nano. 2009; 4:634–641.

[10]. Gill I, Ballesteros A. Encapsulation of biologicals within silicate, siloxane, and hybrid sol-gel polymers: An efficient and generic approach. J. Am. Chem. Soc. 1998; 120:8587–8598.

[11]. Kong B, Seog JH, Graham LM, Lee SB. Experimental considerations on the cytotoxicity of nanoparticles. Nanomedicine (Lond). 2011; 6:929–941. [PubMed: 21793681]

[12]. Barnard AS. Nanohazards: Knowledge is our first defence. Nat Mater. 2006; 5:245–248. [PubMed: 16582921]

[13]. Li Y, Sun L, Jin M, Du Z, Liu X, Guo C, Li Y, Huang P, Sun Z. Size-dependent cytotoxicity of amorphous silica nanoparticles in human hepatoma HepG2 cells. Toxicology in Vitro. 2011; 25:1343–1352. [PubMed: 21575712]

[14]. Huang X, Li L, Liu T, Hao N, Liu H, Chen D, Tang F. The Shape Effect of Mesoporous Silica Nanoparticles on Biodistribution, Clearance, and Biocompatibility in Vivo. ACS Nano. 2011; 5:5390–5399. [PubMed: 21634407]

[15]. Chung T-H, Wu S-H, Yao M, Lu C-W, Lin Y-S, Hung Y, Mou C-Y, Chen Y-C, Huang D-M. The effect of surface charge on the uptake and biological function of mesoporous silica nanoparticles in 3T3-L1 cells and human mesenchymal stem cells. Biomaterials. 2007; 28:2959–2966. [PubMed: 17397919]

[16]. Stern ST, McNeil SE. Nanotechnology Safety Concerns Revisited. Toxicological Sciences. 2008; 101:4–21. [PubMed: 17602205]

[17]. Bruno G, Capezzuto P, Madan A. Plasma Deposition of Amorphous Silicon-Based Materials. Elsevier Science. 1995

[18]. Sun L, Gong K. Silicon-Based Materials from Rice Husks and Their Applications. Industrial & Engineering Chemistry Research. 2001; 40:5861–5877.

[19]. Nalwa, HS. Silicon-based Materials and Devices. Academic Press; 2001.

[20]. Matsumoto N. Overview of silicon-based materials. Jpn. J. Appl. Phys. Part 1 - Regul. Pap. Short Notes Rev. Pap. 1998; 37:5425–5436.

[21]. Lam CW, James JT, McCluskey R, Hunter RL. Pulmonary toxicity of single-wall carbon nanotubes in mice 7 and 90 days after intratracheal instillation. Toxicological Sciences. 2004; 77:126–134. [PubMed: 14514958]

[22]. Warheit DB, Laurence BR, Reed KL, Roach DH, Reynolds GAM, Webb TR. Comparative pulmonary toxicity assessment of single-wall carbon nanotubes in rats. Toxicological Sciences. 2004; 77:117–125. [PubMed: 14514968]

[23]. Muller J, Huaux F, Moreau N, Misson P, Heilier JF, Delos M, Arras M, Fonseca A, Nagy JB, Lison D. Respiratory toxicity of multi-wall carbon nanotubes. Toxicol. Appl. Pharmacol. 2005; 207:221–231. [PubMed: 16129115]

[24]. Davoren M, Herzog E, Casey A, Cottineau B, Chambers G, Byrne HJ, Lyng FM. In vitro toxicity evaluation of single walled carbon nanotubes on human A549 lung cells. Toxicology in Vitro. 2007; 21:438–448. [PubMed: 17125965]

[25]. Smith CJ, Shaw BJ, Handy RD. Toxicity of single walled carbon nanotubes to rainbow trout, (Oncorhynchus mykiss): Respiratory toxicity, organ pathologies, and other physiological effects. Aquat. Toxicol. 2007; 82:94–109. [PubMed: 17343929]

[26]. Murray AR, Kisin E, Leonard SS, Young SH, Kommineni C, Kagan VE, Castranova V, Shvedova AA. Oxidative stress and inflammatory response in dermal toxicity of single-walled carbon nanotubes. Toxicology. 2009; 257:161–171. [PubMed: 19150385]

[27]. Teo BK, Sun XH. Silicon-Based Low-Dimensional Nanomaterials and Nanodevices. Chemical Reviews. 2007; 107:1454–1532. [PubMed: 17488056]

[28]. Okamoto H, Sugiyama Y, Nakano H. Synthesis and Modification of Silicon Nanosheets and Other Silicon Nanomaterials. Chemistry – A European Journal. 2011; 17:9864–9887.

[29]. Anglin EJ, Schwartz MP, Ng VP, Perelman LA, Sailor MJ. Engineering the Chemistry and Nanostructure of Porous Silicon Fabry-Pérot Films for Loading and Release of a Steroid. Langmuir. 2004; 20:11264–11269. [PubMed: 15568884]

[30]. Magarshak, Y.; Kozyrev, S.; Vaseashta, A. Silicon versus carbon : fundamental nanoprocesses, nanobiotechnology and risks assessment. Springer; Dordrecht: 2009.

[31]. Erogbogbo F, Yong KT, Roy I, Xu G, Prasad PN, Swihart MT. Biocompatible luminescent silicon quantum dots for imaging of cancer cells. ACS Nano. 2008; 2:873–878. [PubMed: 19206483]

[32]. van Buuren T, Dinh LN, Chase LL, Siekhaus WJ, Terminello LJ. Changes in the Electronic Properties of Si Nanocrystals as a Function of Particle Size. Physical Review Letters. 1998; 80:3803–3806.

[33]. Littau KA, Szajowski PJ, Muller AJ, Kortan AR, Brus LE. A luminescent silicon nanocrystal colloid via a high-temperature aerosol reaction. The Journal of Physical Chemistry. 1993; 97:1224–1230.

[34]. Wilson WL, Szajowski PF, Brus LE. Quantum Confinement in Size-Selected, Surface-Oxidized Silicon Nanocrystals. Science. 1993; 262:1242–1244. [PubMed: 17772645]

[35]. Takagi H, Ogawa H, Yamazaki Y, Ishizaki A, Nakagiri T. Quantum size effects on photoluminescence in ultrafine Si particles. Applied Physics Letters. 1990; 56:2379–2380.

[36]. Ehbrecht M, Kohn B, Huisken F, Laguna MA, Paillard V. Photoluminescence and resonant Raman spectra of silicon films produced by size-selected cluster beam deposition. Physical Review B. 1997; 56:6958–6964.

[37]. Ledoux G, Gong J, Huisken F, Guillois O, Reynaud C. Photoluminescence of size-separated silicon nanocrystals: Confirmation of quantum confinement. Applied Physics Letters. 2002; 80:4834–4836.

[38]. Botti S, Coppola R, Gourbilleau F, Rizk R. Photoluminescence from silicon nano-particles synthesized by laser-induced decomposition of silane. Journal of Applied Physics. 2000; 88:3396–3401.

[39]. Borsella E, Falconieri M, Botti S, Martelli S, Bignoli F, Costa L, Grandi S, Sangaletti L, Allieri B, Depero L. Optical and morphological characterization of Si nanocrystals/silica composites prepared by sol–gel processing. Materials Science and Engineering: B. 2001; 79:55–62.

[40]. Li X, He Y, Talukdar SS, Swihart MT. Process for Preparing Macroscopic Quantities of Brightly Photoluminescent Silicon Nanoparticles with Emission Spanning the Visible Spectrum. Langmuir. 2003; 19:8490–8496.

[41]. Heath JR. A Liquid-Solution-Phase Synthesis of Crystalline Silicon. Science. 1992; 258:1131–1133. [PubMed: 17789084]

[42]. Baldwin RK, Zou J, Pettigrew KA, Yeagle GJ, Britt RD, Kauzlarich SM. The preparation of a phosphorus doped silicon film from phosphorus containing silicon nanoparticles. Chemical Communications. 2006:658–660. [PubMed: 16446842]

[43]. Baldwin RK, Pettigrew KA, Garno JC, Power PP, Liu G.-y. Kauzlarich SM. Room Temperature Solution Synthesis of Alkyl-Capped Tetrahedral Shaped Silicon Nanocrystals. J. Am. Chem. Soc. 2002; 124:1150–1151. [PubMed: 11841266]

[44]. Stöber W, Fink A, Bohn E. Controlled growth of monodisperse silica spheres in the micron size range. Journal of Colloid and Interface Science. 1968; 26:62–69.

[45]. Ow H, Larson DR, Srivastava M, Baird BA, Webb WW, Wiesner U. Bright and Stable Core–Shell Fluorescent Silica Nanoparticles. Nano Letters. 2004; 5:113–117. [PubMed: 15792423]

[46]. Burns AA, Vider J, Ow H, Herz E, Penate-Medina-Medina O, Baumgart M, Larson SM, Wiesner U, Bradbury M. Fluorescent Silica Nanoparticles with Efficient Urinary Excretion for Nanomedicine. Nano Letters. 2008; 9:442–448. [PubMed: 19099455]

[47]. Benezra M, Penate-Medina O, Zanzonico PB, Schaer D, Ow H, Burns A, DeStanchina E, Longo V, Herz E, Iyer S, Wolchok J, Larson SM, Wiesner U, Bradbury MS. Multimodal silica nanoparticles are effective cancer-targeted probes in a model of human melanoma. J Clin Invest. 2011; 121:2768–2780. [PubMed: 21670497]

[48]. Osseo-Asare K, Arriagada FJ. Preparation of SiO2 nanoparticles in a non-ionic reverse micellar system. Colloids and Surfaces. 1990; 50:321–339.

[49]. Arriagada FJ, Osseo-Asare K. Synthesis of Nanosize Silica in a Nonionic Water-in-Oil Microemulsion: Effects of the Water/Surfactant Molar Ratio and Ammonia Concentration. J Colloid Interface Sci. 1999; 211:210–220. [PubMed: 10049537]

[50]. Alexandre M, Dubois P. Polymer-layered silicate nanocomposites: preparation, properties and uses of a new class of materials. Materials Science and Engineering: R: Reports. 2000; 28:1–63.

[51]. Wen LX, Ding HM, Wang JX, Chen JF. Porous hollow silica nanoparticles as carriers for controlled delivery of ibuprofen to small intestine. J Nanosci Nanotechnol. 2006; 6:3139–3144. [PubMed: 17048529]

[52]. Chang J-S, Chang KLB, Hwang D-F, Kong Z-L. In Vitro Cytotoxicitiy of Silica Nanoparticles at High Concentrations Strongly Depends on the Metabolic Activity Type of the Cell Line. Environmental Science & Technology. 2007; 41:2064–2068. [PubMed: 17410806]

[53]. Caruso F, Spasova M, Susha A, Giersig M, Caruso RA. Magnetic nanocomposite particles and hollow spheres constructed by a sequential layering approach. Chem. Mat. 2001; 13:109–116.

[54]. Correa-Duarte MA, Giersig M, Kotov NA, Liz-Marzan LM. Control of packing order of self-assembled monolayers of magnetite nanoparticles with and without SiO(2) coating by microwave irradiation. Langmuir. 1998; 14:6430–6435.

[55]. Caruso F, Spasova M, Saigueirino-Maceira V, Liz-Marzan LM. Multilayer assemblies of silica-encapsulated gold nanoparticles on decomposable colloid templates. Advanced Materials. 2001; 13:1090.

[56]. Aslan K, Wu M, Lakowicz JR, Geddes CD. Fluorescent core-shell Ag@SiO2 nanocomposites for metal-enhanced fluorescence and single nanoparticle sensing platforms. J. Am. Chem. Soc. 2007; 129:1524. [PubMed: 17283994]

[57]. Selvan ST, Patra PK, Ang CY, Ying JY. Synthesis of Silica-Coated Semiconductor and Magnetic Quantum Dots and Their Use in the Imaging of Live Cells. Angewandte Chemie. 2007; 119:2500–2504.

[58]. Whitsitt EA, Barron AR. Silica coated single walled carbon nanotubes. Nano Letters. 2003; 3:775–778.

[59]. Anglin EJ, Cheng L, Freeman WR, Sailor MJ. Porous silicon in drug delivery devices and materials. Adv Drug Deliv Rev. 2008; 60:1266–1277. [PubMed: 18508154]

[60]. Qian KK, Bogner RH. Application of mesoporous silicon dioxide and silicate in oral amorphous drug delivery systems. Journal of Pharmaceutical Sciences. 2012; 101:444–463. [PubMed: 21976048]

[61]. Slowing JL II, Vivero-Escoto CW, Wu VS. Lin, Mesoporous silica nanoparticles as controlled release drug delivery and gene transfection carriers. Adv Drug Deliv Rev. 2008; 60:1278–1288. [PubMed: 18514969]

[62]. Uhlir A. ELECTROLYTIC SHAPING OF GERMANIUM AND SILICON. Bell System Technical Journal. 1956; 35:333–347.

[63]. Canham LT, Reeves CL, Loni A, Houlton MR, Newey JP, Simons AJ, Cox TI. Calcium phosphate nucleation on porous silicon: factors influencing kinetics in acellular simulated body fluids. Thin Solid Films. 1997; 297:304–307.

[64]. Jugdaohsingh R, Anderson SH, Tucker KL, Elliott H, Kiel DP, Thompson RP, Powell JJ. Dietary silicon intake and absorption. Am J Clin Nutr. 2002; 75:887–893. [PubMed: 11976163]

[65]. Godin B, Gu J, Serda RE, Bhavane R, Tasciotti E, Chiappini C, Liu X, Tanaka T, Decuzzi P, Ferrari M. Tailoring the degradation kinetics of mesoporous silicon structures through PEGylation. Journal of Biomedical Materials Research Part A. 2010 in press.

[66]. Whitehead MA, Fan D, Mukherjee P, Akkaraju GR, Canham LT, Coffer JL. High-porosity poly(epsilon-caprolactone)/mesoporous silicon scaffolds: calcium phosphate deposition and biological response to bone precursor cells. Tissue Eng Part A. 2008; 14:195–206. [PubMed: 18333817]

[67]. Alvarez SD, Derfus AM, Schwartz MP, Bhatia SN, Sailor MJ. The compatibility of hepatocytes with chemically modified porous silicon with reference to in vitro biosensors. Biomaterials. 2009; 30:26–34. [PubMed: 18845334]

[68]. Moxon KA, Hallman S, Aslani A, Kalkhoran NM, Lelkes PI. Bioactive properties of nanostructured porous silicon for enhancing electrode to neuron interfaces. J Biomater Sci Polym Ed. 2007; 18:1263–1281. [PubMed: 17939885]

[69]. Hu L, Xu S, Pan C, Zou H, Jiang G. Preparation of a biochip on porous silicon and application for label-free detection of small molecule-protein interactions. Rapid Commun Mass Spectrom. 2007; 21:1277–1281. [PubMed: 17342786]

[70]. Charnay C, Begu S, Tourne-Peteilh C, Nicole L, Lerner DA, Devoisselle JM. Inclusion of ibuprofen in mesoporous templated silica: drug loading and release property. Eur J Pharm Biopharm. 2004; 57:533–540. [PubMed: 15093603]

[71]. Coffer JL, Montchamp J-L, Aimone JB, Weis RP. Routes to calcified porous silicon: implications for drug delivery and biosensing. physica status solidi (a). 2003; 197:336–339.

[72]. Vaccari L, Canton D, Zaffaroni N, Villa R, Tormen M, di Fabrizio E. Porous silicon as drug carrier for controlled delivery of doxorubicin anticancer agent. Microelectronic Engineering. 2006; 83:1598–1601.

[73]. Rosenholm JM, Linden M. Towards establishing structure-activity relationships for mesoporous silica in drug delivery applications. J Control Release. 2008; 128:157–164. [PubMed: 18439699]

[74]. Godin B, Tasciotti E, Liu X, Serda RE, Ferrari M. Multistage Nanovectors: From Concept to Novel Imaging Contrast Agents and Therapeutics. Acc Chem Res. 2011

[75]. Fan J, Fang G, Wang X, Zeng F, Xiang Y, Wu S. Targeted anticancer prodrug with mesoporous silica nanoparticles as vehicles. Nanotechnology. 2011; 22:455102. [PubMed: 22019849]

[76]. Meade SO, Yoon MS, Ahn KH, Sailor MJ. Porous Silicon Photonic Crystals as Encoded Microcarriers. Advanced Materials. 2004; 16:1811–1814.

[77]. Park JH, Gu L, von Maltzahn G, Ruoslahti E, Bhatia SN, Sailor MJ. Biodegradable luminescent porous silicon nanoparticles for in vivo applications. Nat Mater. 2009; 8:331–336. [PubMed: 19234444]

[78]. Salonen J, Laitinen L, Kaukonen AM, Tuura J, Bjorkqvist M, Heikkila T, Vaha-Heikkila K, Hirvonen J, Lehto VP. Mesoporous Silicon Microparticles for Oral Drug Delivery: Loading and Release of Five Model Drugs. J Control Release. 2005; 108:362–374. [PubMed: 16169628]

[79]. Chiappini C, Tasciotti E, Fakhoury JR, Fine D, Pullan L, Wang YC, Fu L, Liu X, Ferrari M. Tailored porous silicon microparticles: fabrication and properties. Chemphyschem. 2010; 11:1029–1035. [PubMed: 20162656]

[80]. Tasciotti E, Liu X, Bhavane R, Plant K, Leonard AD, Price BK, Cheng MM-C, Decuzzi P, Tour JM, Robertson F, Ferrari M. Mesoporous silicon particles as a multistage delivery system for imaging and therapeutic applications. Nat Nano. 2008; 3:151–157.

[81]. Tanaka T, Godin B, Bhavane R, Nieves-Alicea R, Gu J, Liu X, Chiappini C, Fakhoury JR, Amra S, Ewing A, Li Q, Fidler IJ, Ferrari M. In vivo evaluation of safety of nanoporous silicon carriers following single and multiple dose intravenous administrations in mice. Int. J. Pharm. 2010; 402:190–197. [PubMed: 20883755]

[82]. Serda RE, Godin B, Blanco E, Chiappini C, Ferrari M. Multi-stage delivery nano-particle systems for therapeutic applications. Biochim Biophys Acta. 2011; 1810:317–329. [PubMed: 20493927]

[83]. Godin B, Tasciotti E, Liu X, Serda RE, Ferrari M. Multistage nanovectors: from concept to novel imaging contrast agents and therapeutics. Acc Chem Res. 2011; 44:979–989. [PubMed: 21902173]

[84]. Decuzzi P, Godin B, Tanaka T, Lee SY, Chiappini C, Liu X, Ferrari M. Size and Shape Effects in the Biodistribution of Intravascularly Injected Particles. J Control Release. 2010; 141:320–327. [PubMed: 19874859]

[85]. Lee JE, Lee N, Kim T, Kim J, Hyeon T. Multifunctional Mesoporous Silica Nanocomposite Nanoparticles for Theranostic Applications. Accounts of Chemical Research. 2011; 44:893–902. [PubMed: 21848274]

[86]. Salonen J, Lehto V-P. Fabrication and chemical surface modification of mesoporous silicon for biomedical applications. Chemical Engineering Journal. 2008; 137:162–172.

[87]. Halimaoui A, Oules C, Bomchil G, Bsiesy A, Gaspard F, Herino R, Ligeon M, Muller F. Electroluminescence in the visible range during anodic oxidation of porous silicon films. Applied Physics Letters. 1991; 59:304–306.

[88]. Zhang LZ, Zong BQ, Zhang BR, Xu ZH, Li JQ, Qin GG. Photoluminescence peak energy evolution for porous silicon during photo-oxidation and gamma -ray oxidation. Journal of Physics: Condensed Matter. 1995; 7:697.

[89]. Li K-H, Tsai C, Campbell JC, Hance BK, White JM. Investigation of rapid-thermal-oxidized porous silicon. Applied Physics Letters. 1993; 62:3501–3503.

[90]. Salonen J, Lehto V-P, Laine E. Thermal oxidation of free-standing porous silicon films. Applied Physics Letters. 1997; 70:637–639.

[91]. Hurley PT, Ribbe AE, Buriak JM. Nanopatterning of Alkynes on Hydrogen-Terminated Silicon Surfaces by Scanning Probe-Induced Cathodic Electrografting. J. Am. Chem. Soc. 2003; 125:11334–11339. [PubMed: 16220956]

[92]. Holland JM, Stewart MP, Allen MJ, Buriak JM. Metal Mediated Reactions on Porous Silicon Surfaces. Journal of Solid State Chemistry. 1999; 147:251–258.

[93]. Buriak JM. Organometallic chemistry on silicon surfaces: formation of functional monolayers bound through Si-C bonds. Chemical Communications. 1999:1051–1060.

[94]. Salonen J, Laine E, Niinisto L. Thermal carbonization of porous silicon surface by acetylene. Journal of Applied Physics. 2002; 91:456–461.

[95]. Hilliard LR, Zhao X, Tan W. Immobilization of oligonucleotides onto silica nanoparticles for DNA hybridization studies. Analytica Chimica Acta. 2002; 470:51–56.

[96]. Qhobosheane M, Santra S, Zhang P, Tan W. Biochemically functionalized silica nanoparticles. Analyst. 2001; 126:1274–1278. [PubMed: 11534592]

[97]. Schlossbauer A, Kecht J, Bein T. Biotin-Avidin as a Protease-Responsive Cap System for Controlled Guest Release from Colloidal Mesoporous Silica. Angew. Chem.-Int. Edit. 2009; 48:3092–3095.

[98]. Sadasivan S, Sukhorukov GB. Fabrication of hollow multifunctional spheres containing MCM-41 nanoparticles and magnetite nanoparticles using layer-by-layer method. Journal of Colloid and Interface Science. 2006; 304:437–441. [PubMed: 17010361]

[99]. Godin, B.; Touitou, E. Nanoparticles aiming at specific targets - dermal and transdermal delivery. In: Domb, AJ.; Tabata, Y.; Ravi Kumar, MNV.; Farber, S., editors. Nanoparticles for Pharmaceutical Applications. American Scientific Publishers; Valencia: 2007.

[100]. Godin B, Gu J, Serda RE, Liu X, Ferrati S, Chiappini C, Tanaka T, Decuzzi P, Ferrari M. Multistage mesoporous silicon-based nanocarriers: biocompatibility and controlled degradation in physiological fluids. Controll Release Newsl. 2008; 25:9–11. [PubMed: 21853161]

[101]. Serda RE, Mack A, Pulikkathara M, Zaske AM, Chiappini C, Fakhoury JR, Webb D, Godin B, Conyers JL, Liu XW, Bankson JA, Ferrari M. Cellular association and assembly of a multistage delivery system. Small. 2010; 6:1329–1340. [PubMed: 20517877]

[102]. Tasciotti E, Godin B, Martinez JO, Chiappini C, Bhavane R, Liu X, Ferrari M. Near-infrared imaging method for the in vivo assessment of the biodistribution of nanoporous silicon particles. Mol Imaging. 2011; 10:56–68. [PubMed: 21303615]

[103]. Souza GR, Christianson DR, Staquicini FI, Ozawa MG, Snyder EY, Sidman RL, Miller JH, Arap W, Pasqualini R. Networks of gold nanoparticles and bacteriophage as biological sensors and cell-targeting agents. Proceedings of the National Academy of Sciences of the United States of America. 2006; 103:1215–1220. [PubMed: 16434473]

[104]. Srinivasan, S.; Dressen, WP.; Proneth, B.; Alexander, JF.; Hu, Y.; Liu, X.; Arap, W.; Pasqualini, R.; Ferrari, M. Multifunctional Nanoassemblies: Selective Interactions with Breast Cancer Cells; Controlled Release Soceity Annual Meeting; Maryland; 2011;

[105]. Godin B, Gu J, Serda RE, Bhavane R, Tasciotti E, Chiappini C, Liu X, Tanaka T, Decuzzi P, Ferrari M. Tailoring the degradation kinetics of mesoporous silicon structures through PEGylation. J Biomed Mater Res A. 2010; 94:1236–1243. [PubMed: 20694990]

[106]. Serda RE, Ferrati S, Godin B, Tasciotti E, Liu X, Ferrari M. Mitotic trafficking of silicon microparticles. Nanoscale. 2009; 1:250–259. [PubMed: 20644846]

[107]. Serda RE, Mack A, Pulikkathara M, Zaske AM, Chiappini C, Fakhoury J, Webb D, Godin B, Conyers JL, Liu XW, Bankson JA, Ferrari M. Cellular Association and Assembly of a Multistage Delivery System. Small. 2010

[108]. Serda RE, Mack A, van de Ven AL, Ferrati S, Dunner K Jr. Godin B, Chiappini C, Landry M, Brousseau L, Liu X, et al. Logic-Embedded Vectors for Intracellular Partitioning, Endosomal Escape, and Exocytosis of Nanoparticles. Small. 2010; 6:2691–2700. [PubMed: 20957619]

[109]. Yu T, Malugin A, Ghandehari H. Impact of Silica Nanoparticle Design on Cellular Toxicity and Hemolytic Activity. ACS Nano. 2011; 5:5717–5728. [PubMed: 21630682]

[110]. Xie G, Sun J, Zhong G, Shi L, Zhang D. Biodistribution and toxicity of intravenously administered silica nanoparticles in mice. Archives of Toxicology. 2010; 84:183–190. [PubMed: 19936708]

[111]. Choi J, Zhang Q, Reipa V, Wang NS, Stratmeyer ME, Hitchins VM, Goering PL. Comparison of cytotoxic and inflammatory responses of photoluminescent silicon nanoparticles with silicon micron-sized particles in RAW 264.7 macrophages. J. Appl. Toxicol. 2009; 29:52–60. [PubMed: 18785685]

[112]. Canham, LT. INSPEC (Information service), Properties of porous silicon. INSPEC; London: 1987.

[113]. Napierska D, Thomassen LCJ, Rabolli V, Lison D, Gonzalez L, Kirsch-Volders M, Martens JA, Hoet PH. Size-Dependent Cytotoxicity of Monodisperse Silica Nanoparticles in Human Endothelial Cells. Small. 2009; 5:846–853. [PubMed: 19288475]

[114]. Bauer AT, Strozyk EA, Gorzelanny C, Westerhausen C, Desch A, Schneider MF, Schneider SW. Cytotoxicity of silica nanoparticles through exocytosis of von Willebrand factor and necrotic cell death in primary human endothelial cells. Biomaterials. 2011; 32:8385–8393. [PubMed: 21840590]

[115]. Zhao Y, Sun X, Zhang G, Trewyn BG, Slowing II, Lin VSY. Interaction of Mesoporous Silica Nanoparticles with Human Red Blood Cell Membranes: Size and Surface Effects. ACS Nano. 2011; 5:1366–1375. [PubMed: 21294526]

[116]. Maurer-Jones MA, Lin Y-S, Haynes CL. Functional Assessment of Metal Oxide Nanoparticle Toxicity in Immune Cells. ACS Nano. 2010; 4:3363–3373. [PubMed: 20481555]

[117]. Godin B, Gu J, Serda RE, Bhavane R, Tasciotti E, Chiappini C, Liu X, Tanaka T, Decuzzi P, Ferrari M. Tailoring the degradation kinetics of mesoporous silicon structures through PEGylation. Journal of Biomedical Materials Research Part A. 2010; 94A:1236–1243. [PubMed: 20694990]

[118]. Bimbo LM, Mäkilä E, Laaksonen T, Lehto V-P, Salonen J, Hirvonen J, Santos HA. Drug permeation across intestinal epithelial cells using porous silicon nanoparticles. Biomaterials. 2011; 32:2625–2633. [PubMed: 21194747]

[119]. Sohaebuddin SK, Thevenot PT, Baker D, Eaton JW, Tang L. Nanomaterial cytotoxicity is composition, size, and cell type dependent. Particle and Fibre Toxicology. 7:1–17. [PubMed: 20180970]

[120]. Waters KM, Masiello LM, Zangar RC, Karin NJ, Quesenberry RD, Bandyopadhyay S, Teeguarden JG, Pounds JG, Thrall BD. Macrophage Responses to Silica Nanoparticles are Highly Conserved Across Particle Sizes. Toxicological Sciences. 2009; 107:553–569. [PubMed: 19073995]

[121]. Jeong YS, Oh W-K, Kim S, Jang J. Cellular uptake, cytotoxicity, and ROS generation with silica/conducting polymer core/shell nanospheres. Biomaterials. 2011; 32:7217–7225. [PubMed: 21724253]

[122]. Yuan H, Gao F, Zhang Z, Miao L, Yu R, Zhao H, Lan M. Study on Controllable Preparation of Silica Nanoparticles With Multi-Sizes and Their Size-dependent Cytotoxicity in Phaeochromaocytoma Cells and Human Embroynic Kidney Cells. Water. 2010; 56:632–640.

[123]. Fisichella M, Dabboue H, Bhattacharyya S, Lelong G, Saboungi ML, Warmont F, Midoux P, Pichon C, Guerin M, Hevor T, Salvetat JP. Uptake of functionalized mesoporous silica nanoparticles by human cancer cells. J Nanosci Nanotechnol. 2010; 10:2314–2324. [PubMed: 20355428]

[124]. Di Pasqua AJ, Sharma KK, Shi YL, Toms BB, Ouellette W, Dabrowiak JC, Asefa T. Cytotoxicity of mesoporous silica nanomaterials. J. Inorg. Biochem. 2008; 102:1416–1423. [PubMed: 18279965]

[125]. Al-Rawi M, Diabaté S, Weiss C. Uptake and intracellular localization of submicron and nano-sized SiO₂ particles in HeLa cells. Archives of Toxicology. 2011; 85:813–826. [PubMed: 21240478]

[126]. De Angelis F, Pujia A, Falcone C, Iaccino E, Palmieri C, Liberale C, Mecarini F, Candeloro P, Luberto L, de Laurentiis A, Das G, Scala G, Di Fabrizio E. Water soluble nanoporous nanoparticle for in vivo targeted drug delivery and controlled release in B cells tumor context. Nanoscale. 2010; 2

[127]. Tao Z, Toms BB, Goodisman J, Asefa T. Mesoporosity and Functional Group Dependent Endocytosis and Cytotoxicity of Silica Nanomaterials. Chem. Res. Toxicol. 2009; 22:1869–1880. [PubMed: 19817448]

[128]. Park MVDZ, Annema W, Salvati A, Lesniak A, Elsaesser A, Barnes C, McKerr G, Howard CV, Lynch I, Dawson KA, Piersma AH, Jong W.H.d. In vitro development toxicity test detects inhibition of stem cell differentiation by silica nanoparticles. Toxicol Appl Pharmacol. 2009; 240:108–116. [PubMed: 19631676]

[129]. Ariano P, Zamburlin P, Gilardino A, Mortera R, Onida B, Tomatis M, Ghiazza M, Fubini B, Lovisolo D. Interaction of Spherical Silica Nanoparticles with Neuronal Cells: Size-Dependent Toxicity and Perturbation of Calcium Homeostasis. Small. 2011; 7:766–774. [PubMed: 21302356]

[130]. Drescher D, Orts-Gil G, Laube G, Natte K, Veh R, Österle W, Kneipp J. Toxicity of amorphous silica nanoparticles on eukaryotic cell model is determined by particle agglomeration and serum protein adsorption effects. Analytical and Bioanalytical Chemistry. 2011; 400:1367–1373. [PubMed: 21479547]

[131]. Tanaka T, Mangala LS, Vivas-Mejia PE, Nieves-Alicea R, Mann AP, Mora E, Han HD, Shahzad MM, Liu X, Bhavane R, et al. Sustained Small Interfering RNA Delivery by Mesoporous Silicon Particles. Cancer Res. 2010; 70:3687–3696. [PubMed: 20430760]

[132]. Lu X, Tian Y, Zhao Q, Jin T, Xiao S, Fan X. Integrated metabonomics analysis of the size-response relationship of silica nanoparticles-induced toxicity in mice. Nanotechnology. 2011; 22:055101. [PubMed: 21178262]

[133]. Tanaka T, Godin B, Bhavane R, Nieves-Alicea R, Gu J, Liu X, Chiappini C, Fakhoury JR, Amra S, Ewing A, Li Q, Fidler IJ, Ferrari M. In vivo evaluation of safety of nanoporous silicon carriers following single and multiple dose intravenous administrations in mice. Int J Pharm. 2010; 402:190–197. [PubMed: 20883755]

[134]. Decuzzi P, Godin B, Tanaka T, Lee SY, Chiappini C, Liu X, Ferrari M. Size and shape effects in the biodistribution of intravascularly injected particles. Journal of Controlled Release. 2010; 141:320–327. [PubMed: 19874859]

[135]. He Q, Zhang Z, Gao F, Li Y, Shi J. In vivo Biodistribution and Urinary Excretion of Mesoporous Silica Nanoparticles: Effects of Particle Size and PEGylation. Small. 2011; 7:271–280. [PubMed: 21213393]

[136]. Liu T, Li L, Teng X, Huang X, Liu H, Chen D, Ren J, He J, Tang F. Single and repeated dose toxicity of mesoporous hollow silica nanoparticles in intravenously exposed mice. Biomaterials. 2011; 32:1657–1668. [PubMed: 21093905]

[137]. Bimbo LM, Sarparanta M, Santos H.l.A. Airaksinen AJ, Mäkilä E, Laaksonen T, Peltonen L, Lehto V-P, Hirvonen J, Salonen J. Biocompatibility of Thermally Hydrocarbonized Porous Silicon Nanoparticles and their Biodistribution in Rats. ACS Nano. 2010; 4:3023–3032. [PubMed: 20509673]

[138]. Kumar R, Roy I, Ohulchanskky TY, Vathy LA, Bergey EJ, Sajjad M, Prasad PN. In vivo Biodistribution and Clearance Studies Using Multimodal Organically Modified Silica Nanoparticles. ACS Nano. 2010; 4:699–708. [PubMed: 20088598]

[139]. Cho W-S, Duffin R, Poland CA, Howie SEM, MacNee W, Bradley M, Megson IL, Donaldson K. Metal Oxide Nanoparticles Induce Unique Inflammatory Footprints in the Lung: Important Implications for Nanoparticle Testing. Environ Health Perspect. 2010; 118

[140]. Refuerzo JS, Godin B, Bishop K, Srinivasan S, Shah SK, Amra S, Ramin SM, Ferrari M. Size of the nanovectors determines the transplacental passage in pregnancy: study in rats. American Journal of Obstetrics and Gynecology. 2011; 204:546.e545.e545–546.e549. [PubMed: 21481834]

[141]. Yamashita K, Yoshioka Y, Higashisaka K, Mimura K, Morishita Y, Nozaki M, Yoshida T, Ogura T, Nabeshi H, Nagano K, Abe Y, Kamada H, Monobe Y, Imazawa T, Aoshima H, Shishido K, Kawai Y, Mayumi T, Tsunoda S.-i. Itoh N, Yoshikawa T, Yanagihara I, Saito S, Tsutsumi Y. Silica and titanium dioxide nanoparticles cause pregnancy complications in mice. Nat Nano. 2011; 6:321–328.

[142]. Chen Z, Meng H, Xing GM, Yuan H, Zhao F, Liu R, Chang XL, Gao XY, Wang TC, Jia G, Ye C, Chai ZF, Zhao YL. Age-Related Differences in Pulmonary and Cardiovascular Responses to SiO(2) Nanoparticle Inhalation: Nanotoxicity Has Susceptible Population. Environmental Science & Technology. 2008; 42:8985–8992. [PubMed: 19192829]

[143]. Ding M, Chen F, Shi X, Yucesoy B, Mossman B, Vallyathan V. Diseases caused by silica: mechanisms of injury and disease development. Int Immunopharmacol. 2002; 2:173–182. [PubMed: 11811922]

[144]. Hnizdo E, Vallyathan V. Chronic obstructive pulmonary disease due to occupational exposure to silica dust: a review of epidemiological and pathological evidence. Occup Environ Med. 2003; 60:237–243. [PubMed: 12660371]

[145]. Merget R, Bauer T, Kupper HU, Philippou S, Bauer HD, Breitstadt R, Bruening T. Health hazards due to the inhalation of amorphous silica. Arch Toxicol. 2002; 75:625–634. [PubMed: 11876495]

[146]. Thibodeau MS, Giardina C, Knecht DA, Helble J, Hubbard AK. Silica-induced apoptosis in mouse alveolar macrophages is initiated by lysosomal enzyme activity. Toxicol Sci. 2004; 80:34–48. [PubMed: 15056807]

[147]. Ale-Agha N, Albrecht C, Klotz L-O. Loss of gap junctional intercellular communication in rat lung epithelial cells exposed to carbon or silica-based nanoparticles. Biological Chemistry. 2010:1333. [PubMed: 20868226]

[148]. Akhtar MJ, Ahamed M, Kumar S, Siddiqui H, Patil G, Ashquin M, Ahmad I. Nanotoxicity of pure silica mediated through oxidant generation rather than glutathione depletion in human lung epithelial cells. Toxicology. 2010; 276:95–102. [PubMed: 20654680]

[149]. Lin W, Huang Y.-w. Zhou X-D, Ma Y. In vitro toxicity of silica nanoparticles in human lung cancer cells. Toxicol. Appl. Pharmacol. 2006; 217:252–259. [PubMed: 17112558]

[150]. Lison D, Thomassen LCJ, Rabolli V, Gonzalez L, Napierska D, Seo JW, Kirsch-Volders M, Hoet P, Kirschhock CEA, Martens JA. Nominal and Effective Dosimetry of Silica Nanoparticles in Cytotoxicity Assays. Toxicological Sciences. 2008; 104:155–162. [PubMed: 18400775]

[151]. Sayes CM, Reed KL, Warheit DB. Assessing toxicity of fine and nanoparticles: Comparing in vitro measurements to in vivo pulmonary toxicity profiles. Toxicological Sciences. 2007; 97:163–180. [PubMed: 17301066]

[152]. Barillet S, Jugan M-L, Laye M, Leconte Y, Herlin-Boime N, Reynaud C, Carriere M. In vitro evaluation of SiC nanoparticle impact on A549 pulmonary cells: Cyto-, Genotoxicity and oxidative stress. Toxicology Letters. 2010; 198:324–330. [PubMed: 20655996]

[153]. Shi Y, Yadav S, Wang F, Wang H. Endotoxin Promotes Adverse Effects of Amorphous Silica Nanoparticles On Lung Epithelial Cells In vitro. Journal of Toxicology and Environmental Health, Part A. 2010; 73:748–756. [PubMed: 20391117]

[154]. Al-Salam S, Balhaj G, Al-Hammadi S, Sudhadevi M, Tariq S, Biradar AV, Asefa T, Souid AK. In Vitro Study and Biocompatibility of Calcined Mesoporous Silica Microparticles in Mouse Lung. Toxicological Sciences. 2011; 122:86–99. [PubMed: 21470958]

[155]. Sayes CM, Reed KL, Glover KP, Swain KA, Ostraat ML, Donner EM, Warheit DB. Changing the dose metric for inhalation toxicity studies: short-term study in rats with engineered aerosolized amorphous silica nanoparticles. Inhal Toxicol. 2010; 22:348–354. [PubMed: 20001567]

[156]. Warheit DB, Webb TR, Colvin VL, Reed KL, Sayes CR. Pulmonary bioassay studies with nanoscale and fine-quartz particles in rats: Toxicity is not dependent upon particle size but on surface characteristics. Toxicological Sciences. 2007; 95:270–280. [PubMed: 17030555]

[157]. Kaewamatawong T, Shimada A, Okajima M, Inoue H, Morita T, Inoue K, Takano H. Acute and subacute pulmonary toxicity of low dose of ultrafine colloidal silica particles in mice after intratracheal instillation. Toxicol. Pathol. 2006; 34:958–965. [PubMed: 17178696]

[158]. Song Y, Li X, Wang L, Rojanasakul Y, Castranova V, Li H, Ma J. Nanomaterials in Humans. Toxicol. Pathol. 2011; 39:841–849. [PubMed: 21768271]

[159]. Eskandar NG, Simovic S, Prestidge CA. Nanoparticle coated emulsions as novel dermal delivery vehicles. Curr Drug Deliv. 2009; 6:367–373. [PubMed: 19534710]

[160]. Touitou E. Drug delivery across the skin. Expert Opinion on Biological Therapy. 2002; 2:723–733. [PubMed: 12387671]

[161]. Cevc G, Vierl U. Nanotechnology and the transdermal route: A state of the art review and critical appraisal. J Control Release. 2010; 141:277–299. [PubMed: 19850095]

[162]. Honeywell-Nguyen PL, de Graaff AM, Groenink HW, Bouwstra JA. The in vivo and in vitro interactions of elastic and rigid vesicles with human skin. Biochim Biophys Acta. 2002; 1573:130–140. [PubMed: 12399022]

[163]. Elias, PM.; Ferngold, KR. Skin Barrier. Taylor & Francis Group; New York: 2006.

[164]. Park YH, Kim JN, Jeong SH, Choi JE, Lee SH, Choi BH, Lee JP, Sohn KH, Park KL, Kim MK, Son SW. Assessment of dermal toxicity of nanosilica using cultured keratinocytes, a human skin equivalent model and an in vivo model. Toxicology. 2010; 267:178–181. [PubMed: 19850098]

[165]. Zhang Y, Hu L, Yu D, Gao C. Influence of silica particle internalization on adhesion and migration of human dermal fibroblasts. Biomaterials. 2010; 31:8465–8474. [PubMed: 20701964]

[166]. Nabeshi H, Yoshikawa T, Matsuyama K, Nakazato Y, Arimori A, Isobe M, Tochigi S, Kondoh S, Hirai T, Akase T, Yamashita T, Yamashita K, Yoshida T, Nagano K, Abe Y, Yoshioka Y, Kamada H, Imazawa T, Itoh N, Tsunoda S, Tsutsumi Y. Size-dependent cytotoxic effects of amorphous silica nanoparticles on Langerhans cells. Pharmazie. 2010; 65:199–201. [PubMed: 20383940]

[167]. Nabeshi H, Yoshikawa T, Matsuyama K, Nakazato Y, Tochigi S, Kondoh S, Hirai T, Akase T, Nagano K, Abe Y, Yoshioka Y, Kamada H, Itoh N, Tsunoda S.-i. Tsutsumi Y. Amorphous nanosilica induce endocytosis-dependent ROS generation and DNA damage in human keratinocytes. Particle and Fibre Toxicology. 2011; 8:1. [PubMed: 21235812]

[168]. Boonen J, Baert B, Lambert J, De Spiegeleer B. Skin penetration of silica microparticles. Pharmazie. 2011; 66:463–464. [PubMed: 21699089]

[169]. Graf C, Meinke M, Gao Q, Hadam S, Raabe J, Sterry W, Blume-Peytavi U, Lademann J, Ruhl E, Vogt A. Qualitative detection of single submicron and nanoparticles in human skin by scanning transmission x-ray microscopy. J Biomed Opt. 2009; 14:021015. [PubMed: 19405728]

[170]. Ghouchi Eskandar N, Simovic S, Prestidge CA. Nanoparticle coated submicron emulsions: sustained in-vitro release and improved dermal delivery of all-trans-retinol. Pharm Res. 2009; 26:1764–1775. [PubMed: 19384464]

[171]. Kosmulski M. Compilation of PZC and IEP of sparingly soluble metal oxides and hydroxides from literature. Adv Colloid Interface Sci. 2009; 152:14–25. [PubMed: 19744641]

[172]. Popov AP, Priezzhev AV, Lademann J, Myllyla R. Biophysical mechanisms of modification of skin optical properties in the UV wavelength range with nanoparticles. Journal of Applied Physics. 2009; 105:102035.

[173]. Ramesan RM, Sharma CP. Challenges and Advances in Nanoparticle -based oral Insulin Delivery. Expert Review of Medical Devices. 2009; 6.6:665. [PubMed: 19911877]

[174]. Cheng S-H, Liao W-N, Chen L-M, Lee C-H. pH-controllable release using functionalized mesoporous silica nanoparticles as an oral drug delivery system. Journal of Materials Chemistry. 2011; 21

[175]. Foraker AB, Walczak RJ, Cohen MH, Boiarski TA, Grove CF, Swaan PW. Microfabricated porous silicon particles enhance paracellular delivery of insulin across intestinal Caco-2 cell monolayers. Pharm Res. 2003; 20:110–116. [PubMed: 12608544]

[176]. Tan A, Simovic S, Davey AK, Rades T, Boyd BJ, Prestidge CA. Silica Nanoparticles To Control the Lipase-Mediated Digestion of Lipid-Based Oral Delivery Systems. Molecular Pharmaceutics. 2010; 7:522–532. [PubMed: 20063867]

[177]. Chu Z, Huang Y, Tao Q, Li Q. Cellular Uptake, Evolution, and Excretion of Silica Nanoparticles in Human Cells. Nanoscale. 2011; 3:3291–3299. [PubMed: 21743927]

[178]. Nishimori H, Kondoh M, Isoda K, Tsunoda S.-i. Tsutsumi Y, Yagi K. Silica nanoparticles as hepatotoxicants. European Journal of Pharmaceutics and Biopharmaceutics. 2009; 72:496–501. [PubMed: 19232391]

[179]. Wang F, Hui H, Barnes TJ, Barnett C, Prestidge CA. Oxidized Mesoporous Silicon Microparticles for Improved Oral Delivery of Poorly Soluble Drugs. Molecular Pharmaceutics. 2009; 7:227–236. [PubMed: 19874003]

[180]. Mellaerts R, Mols R, Jammaer JA, Aerts CA, Annaert P, Van Humbeeck J, Van den Mooter G, Augustijns P, Martens JA. Increasing the oral bioavailability of the poorly water soluble drug itraconazole with ordered mesoporous silica. Eur J Pharm Biopharm. 2008; 69:223–230. [PubMed: 18164930]

[181]. Van Speybroeck M, Mols R, Mellaerts R, Thi TD, Martens JA, Van Humbeeck J, Annaert P, Van den Mooter G, Augustijns P. Combined use of ordered mesoporous silica and precipitation inhibitors for improved oral absorption of the poorly soluble weak base itraconazole. Eur J Pharm Biopharm. 2010; 75:354–365. [PubMed: 20420905]

[182]. Salonen J, Laitinen L, Kaukonen AM, Tuura J, Björkqvist M, Heikkilä T, Vähä-Heikkilä K, Hirvonen J, Lehto VP. Mesoporous silicon microparticles for oral drug delivery: Loading and release of five model drugs. Journal of Controlled Release. 2005; 108:362–374. [PubMed: 16169628]

[183]. Heikkila T, Salonen J, Tuura J, Kumar N, Salmi T, Murzin DY, Hamdy MS, Mul G, Laitinen L, Kaukonen AM, Hirvonen J, Lehto VP. Evaluation of mesoporous TCPSi, MCM-41, SBA-15, and TUD-1 materials as API carriers for oral drug delivery. Drug Deliv. 2007; 14:337–347. [PubMed: 17701523]

[184]. Zhang Y, Zhi Z, Jiang T, Zhang J, Wang Z, Wang S. Spherical mesoporous silica nanoparticles for loading and release of the poorly water-soluble drug telmisartan. Journal of Controlled Release. 2010; 145:257–263. [PubMed: 20450945]

[185]. Lee C-H, Lo L-W, Mou C-Y, Yang C-S. Synthesis and Characterization of Positive-Charge Functionalized Mesoporous Silica Nanoparticles for Oral Drug Delivery of an Anti-Inflammatory Drug. Advanced Functional Materials. 2008; 18:3283–3292.

[186]. Albrecht DS, Lee JT, Molby N, Rhodes SD, Dam HM, Siegel JL, Porter LA. Functionalized Porous Silicon in a Simulated Gastrointestinal Tract: Modeling the Biocompatibility of a Monolayer Protected Nanostructured Material. Mater. Res. Soc. Symp. Proc. 2008; 1063

[187]. Tan A, Simovic S, Davey AK, Rades T, Prestidge CA. Silica-lipid hybrid (SLH) microcapsules: a novel oral delivery system for poorly soluble drugs. J Control Release. 2009; 134:62–70. [PubMed: 19013488]

[188]. Uskoković V, Lee PP, Walsh LA, Fischer KE, Desai TA. PEGylated silicon nanowire coated silica microparticles for drug delivery across intestinal epithelium. Biomaterials. 2012; 33:1663–1672. [PubMed: 22116000]

[189]. Laaksonen T, Santos H, Vihola H, Salonen J, Riikonen J, Heikkila T, Peltonen L, Kumar N, Murzin DY, Lehto VP, Hirvonen J. Failure of MTT as a toxicity testing agent for mesoporous silicon microparticles. Chem Res Toxicol. 2007; 20:1913–1918. [PubMed: 17990852]

[190]. Jin Y, Kannan S, Wu M, Zhao JX. Toxicity of Luminescent Silica Nanoparticles to Living Cells. Chemical Research in Toxicology. 2007; 20:1126–1133. [PubMed: 17630705]

[191]. Karlsson HL. The comet assay in nanotoxicology research. Anal Bioanal Chem. 2010; 398:651–666. [PubMed: 20640410]

[192]. Schins RP. Mechanisms of genotoxicity of particles and fibers. Inhal Toxicol. 2002; 14:57–78. [PubMed: 12122560]

[193]. Chen M, von Mikecz A. Formation of nucleoplasmic protein aggregates impairs nuclear function in response to SiO2 nanoparticles. Exp Cell Res. 2005; 305:51–62. [PubMed: 15777787]

[194]. IARC Monographs on the Evaluation of Carcinogenic Risks to Humans. World Health Organization International Agency for Research on Cancer. 1997; 68:1–506.

[195]. Borm PJA, Tran L, Donaldson K. The carcinogenic action of crystalline silica: A review of the evidence supporting secondary inflammation-driven genotoxicity as a principal mechanism. Critical Reviews in Toxicology. 2011; 41:756–770. [PubMed: 21923565]

[196]. Zhang Z, Shen H-M, Zhang Q-F, Ong C-N. Involvement of Oxidative Stress in Crystalline Silica-Induced Cytotoxicity and Genotoxicity in Rat Alveolar Macrophages. Environmental Research. 2000; 82:245–253. [PubMed: 10702332]

[197]. Wang JJ, Sanderson BJ, Wang H. Cytotoxicity and genotoxicity of ultrafine crystalline SiO2 particulate in cultured human lymphoblastoid cells. Environ Mol Mutagen. 2007; 48:151–157. [PubMed: 17285640]

[198]. Gerloff K, Albrecht C, Boots AW, Förster I, Schins RPF. Cytotoxicity and oxidative DNA damage by nanoparticles in human intestinal Caco-2 cells. Nanotoxicology. 2009; 3:355–364.

[199]. Choi H-S, Kim Y-J, Song M, Song M-K, Ryu J-C. Genotoxicity of nano-silica in mammalian cell lines. Toxicology and Environmental Health Sciences. 2011; 3:7–13.

[200]. Gong C, Tao G, Yang L, Liu J, Liu Q, Zhuang Z. SiO2 nanoparticles induce global genomic hypomethylation in HaCaT cells. Biochemical and Biophysical Research Communications. 2010; 397:397–400. [PubMed: 20501321]

[201]. Huang X, Zhuang J, Teng X, Li L, Chen D, Yan X, Tang F. The promotion of human malignant melanoma growth by mesoporous silica nanoparticles through decreased reactive oxygen species. Biomaterials. 2010; 31:6142–6153. [PubMed: 20510446]

[202]. arnes CA, Elsaesser A, Arkusz J, Smok A, Palus J, Le niak A, Salvati A, Hanrahan JP, ong W.H.d. Dziubaltowska E.b. Stępnik M, ydzyński K, McKerr G, Lynch I, Dawson KA, Howard

CV. Reproducible Comet Assay of Amorphous Silica Nanoparticles Detects No Genotoxicity. Nano Letters. 2008; 8:3069–3074. [PubMed: 18698730]

[203]. Park MV, Verharen HW, Zwart E, Hernandez LG, van Benthem J, Elsaesser A, Barnes C, McKerr G, Howard CV, Salvati A, Lynch I, Dawson KA, de Jong WH. Genotoxicity evaluation of amorphous silica nanoparticles of different sizes using the micronucleus and the plasmid lacZ gene mutation assay. Nanotoxicology. 2011; 5:168–181. [PubMed: 20735203]

[204]. Aillon KL, Xie Y, El-Gendy N, Berkland CJ, Forrest ML. Effects of nanomaterial physicochemical properties on in vivo toxicity. Adv Drug Deliv Rev. 2009; 61:457–466. [PubMed: 19386275]

[205]. Yang H, Liu C, Yang D, Zhang H, Xi Z. Comparative study of cytotoxicity, oxidative stress and genotoxicity induced by four typical nanomaterials: the role of particle size, shape and composition. J Appl Toxicol. 2009; 29:69–78. [PubMed: 18756589]

[206]. Durnev AD, Solomina AS, Daugel-Dauge NO, Zhanataev AK, Shreder ED, Nemova EP, Shreder OV, Veligura VA, Osminkina LA, Timoshenko VY, Seredenin SB. Evaluation of genotoxicity and reproductive toxicity of silicon nanocrystals. Bull Exp Biol Med. 2010; 149:445–449. [PubMed: 21234440]

[207]. Kneuer C, Sameti M, Bakowsky U, Schiestel T, Schirra H, Schmidt H, Lehr CM. A nonviral DNA delivery system based on surface modified silica-nanoparticles can efficiently transfect cells in vitro. Bioconjugate Chem. 2000; 11:926–932.

[208]. Ravi Kumar MNV, Sameti M, Mohapatra SS, Kong X, Lockey RF, Bakowsky U, Lindenblatt G, Schmidt H, Lehr CM. Cationic silica nanoparticles as gene carriers: synthesis, characterization and transfection efficiency in vitro and in vivo. Journal of nanoscience and nanotechnology. 2004; 4:876–881. [PubMed: 15570975]

[209]. Xue Z-G, Zheng D, Ruan J-M, Pan Q, Zhao D-C, Liu X-P, Chen Y-X, Xia J-H, Xia K. Silica nanoparticles modified as carriers for gene transfection. Yi chuan xue bao = Acta genetica Sinica. 2003; 30:606–610. [PubMed: 14579527]

[210]. Zhang HY, Lee MY, Hogg MG, Dordick JS, Sharfstein ST. Gene Delivery in Three-Dimensional Cell Cultures by Superparamagnetic Nanoparticles. ACS Nano. 2010; 4:4733–4743. [PubMed: 20731451]

[211]. Ciofani G, Ricotti L, Menciassi A, Mattoli V. Preparation, characterization and in vitro testing of poly(lactic-co-glycolic) acid/barium titanate nanoparticle composites for enhanced cellular proliferation. Biomed. Microdevices. 2011; 13:255–266. [PubMed: 20981490]

[212]. Child HW, del Pino PA, De la Fuente JM, Hursthouse AS, Stirling D, Mullen M, McPhee GM, Nixon C, Jayawarna V, Berry CC. Working Together: The Combined Application of a Magnetic Field and Penetratin for the Delivery of Magnetic Nanoparticles to Cells in 3D. ACS Nano. 2011; 5:7910–7919. [PubMed: 21894941]

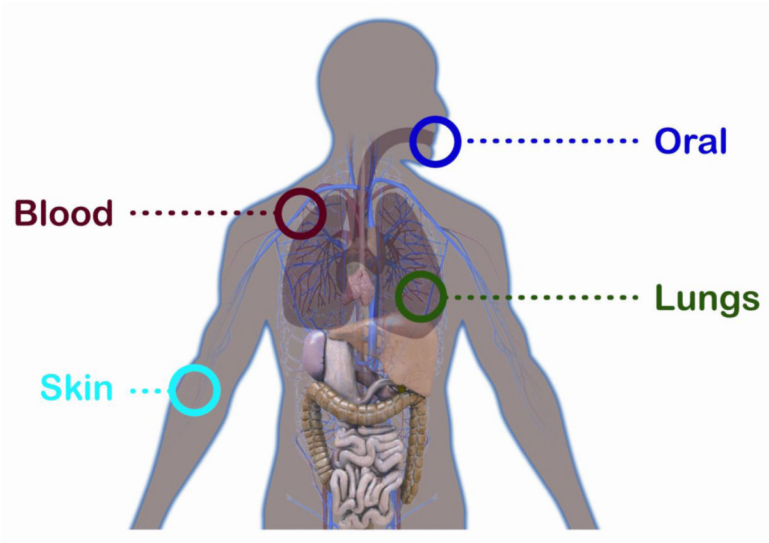

Fig. 1.
Schematic presentation of various exposure/drug delivery routes discussed in this review.

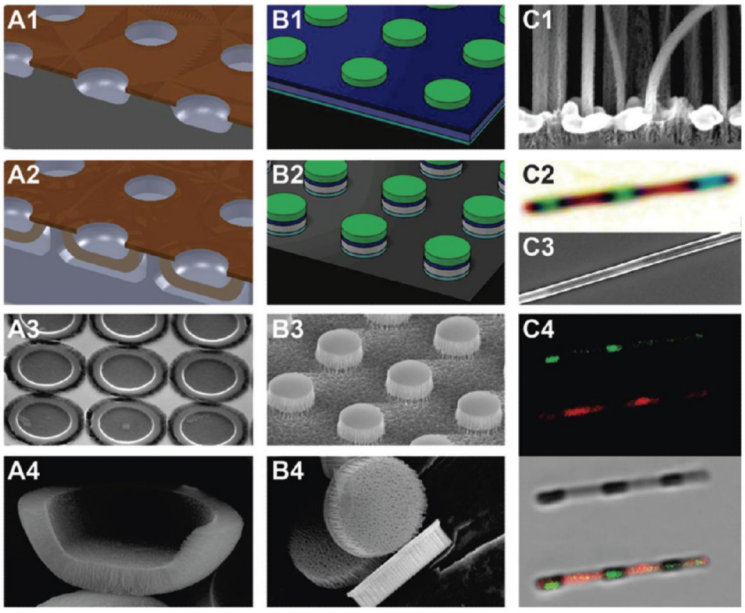

Fig. 2.

Fabrication of pSi micron and submicron size particles by photolithography and electrochemical etching. A1: Patterned SiN layer and trenches etched into Si wafer. A2: Electrochemically etched pSi particles with release layer. A3: Example pSi particles array on wafer after removal of SiN. A4: Cross-section of quasi-hemispherical pSi. B1: Photoresist pattern on LTO capped pSi film with release layer. B2: Particle array on wafer after RIE. B3: Example discoidal pSi particle array on wafer after LTO removal. B4: Released discoidal pSi particles. C1: Silver nanopattern etched into Si forming pSi nanowires. C2: Nanowire barcode under white light. C3: SEM image of nanowire barcode. C4: 3-channel confocal microscopy images of nanowire barcode with green Q-dot loaded in small pore segment and red Q-dot in bigger pore segment. Reproduced from Godin *et al.* [74] with permission from ACS publications.

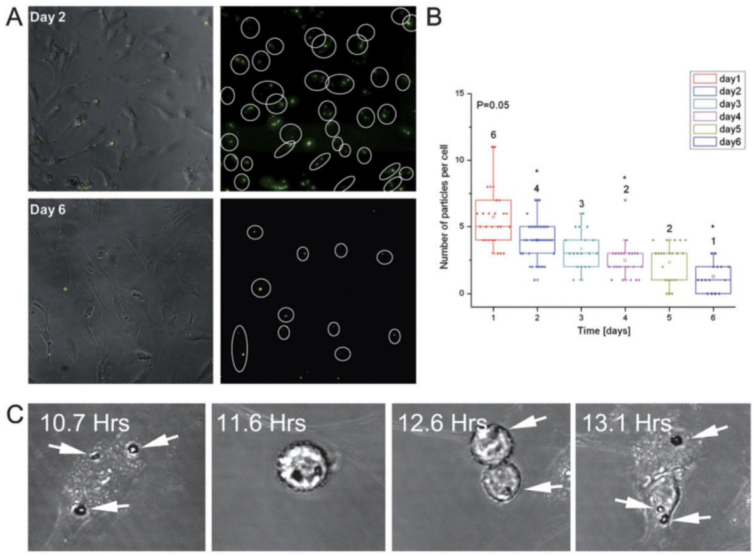

Fig. 3.

Quantification of pSi microparticles per cell during multiple mitotic events. HMVECs were incubated with fluorescent pSi particles, then FACS-sorted to obtain a homogeneous population of cells with similar numbers of internalized pSi particles. A) Representative phase contrast and fluorescent microscope images of HMVECs at day 2 and day 6 following pSi particle internalization. B) Statistical box charts displaying the number of pSi particles per cell with time. The graphs show the 25th, 75th (box range), and 50th (middle line) percentiles, as well as the average number of particles per cell (small open square and number on top of box). Populations that differ significantly from the preceding significant time point are marked by a star. C) Dividing cell with internalized 3.2 μm pSi particles monitored by phase contrast and live confocal microscopy. Reprinted from Serda *et al[106]* with permission from Royal Society of Chemistry.

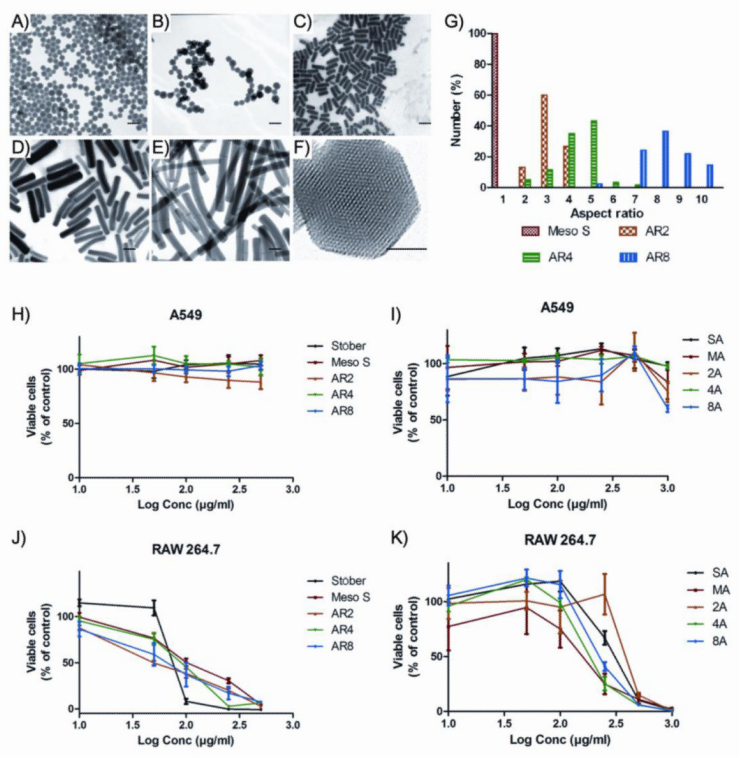

Fig. 4.

Transmission electron microscopy images of (A) Stöber SiO_2 with average diameter of 115 nm (referred to as Stöber), (B) mesoporous SiO_2 with average diameter of 120 nm (Meso S), (C) mesoporous pSiO nanorods with aspect ratio 2 (AR2), (D) mesoporous pSiO nanorods with aspect ratio 4 (AR4), (E) mesoporous pSi nanorods with aspect ratio 8 (AR8), and (F) high-resolution image of a single particle in B. Scale bars in A–E = 200 nm, scale bar in F = 50 nm. (G) Percentage distribution histogram as a function of aspect ratio. Proliferation inhibition assay of adenocarcinomic human alveolar basal epithelial cells A549 (H, I) and RAW 264.7 macrophages (J, K) cells after continuous 72 h incubation with bare (H, J) and amine-modified (I, K) SiO_2. Data are mean ± SD (n = 3). Reprinted from Yu *et al.* [109]with permission from ACS

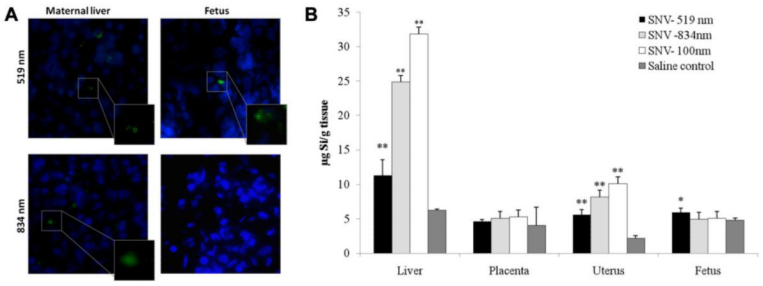

Fig. 5.

(A) Visualization of fluorescently labeled SiO particles of two different sizes in placenta and fetus; (B) Comparison of Si concentration (microgram of Si per gram tissue) in liver, uterus and placenta of pregnant rats, as well as, in fetal tissues as a function of size. SNV- SiO nanovectors; NS- not significant; **= $p<0.01$ vs. control. From Refuerzo, Godin *et al.*[140] with permission from Elsevier.

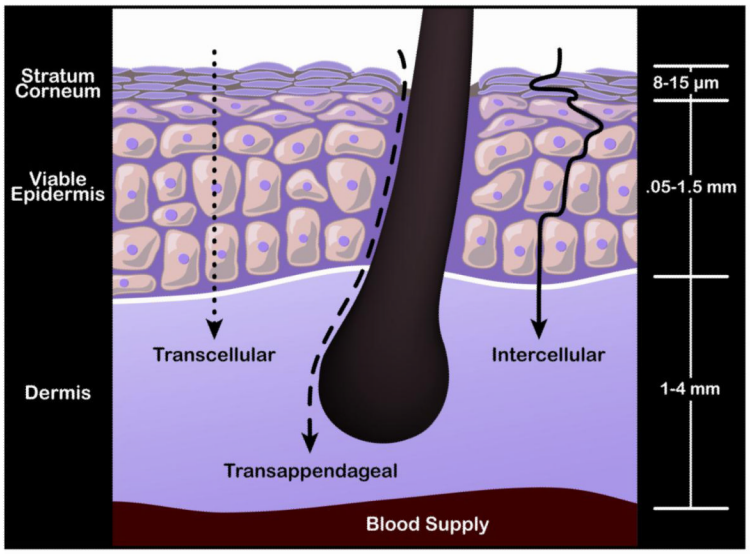

Fig. 6.
Schematic presentation of the skin structure and routes for permeation of the agent applied to the skin surface and to the viable layers across the skin: intercellular, transappendageal and transcellular routes.

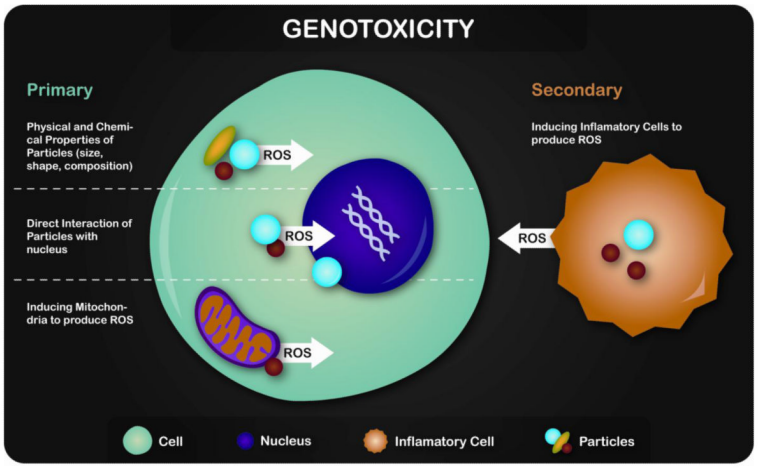

Fig. 7.
Schematic presentation of primary and secondary mechanisms of genotoxicity mechanisms that can be induced by particles.

Table 1

Chemical bond lengths in silicon- and carbon-containing compounds (compiled from Ref. [30]).

Si		C		Delta (Si-C)
Bond	**Length (Å)**	**Bond**	**Length (Å)**	
Si-O	1.63	C-O	1.41	0.22
Si-C	1.89	C-C	1.54	0.35
Si-H	1.42	C-H	1.09	0.39
Si-Si	2.29	Si-C	1.89	0.40
Si-Cl	2.05	C-Cl	1.78	0.27
Si-N	1.74	C-N	1.47	0.35

Table 2

In vitro studies on interactions of Si and SiO particles with endothelial cells.

Type of Particle	Size of Particle	Cells	Assay	Dosage	Treatment time (h)	Conclusions	Ref
Amorphous spherical Si	14 – 60 nm	Endothelial cells (EAHY926)	LDH and MTT	0 – 2500 μg/ml	1 – 24	Cell viability and LDH release decreased 50% at NP concentrations greater than 50 μg/ml after 24 h	[113]
Amorphous spherical SiO	104 - 335 nm	Endothelial cells (EAHY926)	LDH and MTT	0 – 2500 μg/ml	1 – 24	Cell viability and LDH release decreased 50% at NP concentrations greater than 1000 μg/ml after 24 h	[113]
SiO NPs	16 – 304 nm	Human Umbilical Cord Endothelial Cells (HUVEC)	MTT and LDH	1000 to 30000 NPs/cell	24, 48	Cell viability decreased 50% for NP sizes of 212 and 304 nm at concentrations greater than 15000 NPs/cells after 24 and 48 hrs. LDH release increased for 212 and 304 nm sized NPs after 48 h	[114]
pSi microparticles	1.6 or 3.2 μm	HUVEC	MTT	5-10 particles/ cell	24 – 72	No change in cell proliferation compared to control cells for ratios 1:5 and 1:10 cells: particles, normal mitosis and no inflammatory cytokines production	[106]

Table 3

In vitro studies on interactions of Si and SiO particles with whole blood/red blood cells (RBC).

Type of Particle	Size of Particle	Cells	Assay	Dosage	Treatment time (h)	Conclusions	Ref
Mesoporous pSiO spheres and nanorods	120 nm and Aspect ratio of 2, 4, 8	Human RBC	ICP-MS, WST-1	Up to 500 μg/ml	24	Hemolysis for bare SiO NP at concentrations greater than 250 μg/ml and for amine-modified SiO NPs at concentrations greater than 100 μg/ml. Geometry did not influence the extent of cellular association of NPs.	[14]
Mesoporous pSiO NPs (MCM-41)	100 nm	Human RBC	Hemolysis activity	50 and 100 μg/ml	2	No RBC disruption	[115]
Mesoporous pSiO NPs (SBA-15)	600 nm	Human RBC	Hemolysis activity	50 and 100 μg/ml	2	Induced membrane deformation in RBCs and hemolysis	[115]
Mesoporous pSiO NPs	25 ± 4 nm	Human RBC and mast cells	Monitoring hemolysis and MTT	0 – 400 μg/ml	24	No influence on cell viability. Hemolysis at concentrations greater than 270 μg/ml	[116]
Mesoporous pSiO NPs	100 – 300 nm & pore 3 nm	Rabbit RBC	UV – vis absorption spectroscopy	25 – 125 μg/ cm^3	2	10% increase in hemolysis between concentrations of 20 and 100 μg/ml	[61]
Porous and nonporous SiO	19 – 263 nm	Human whole blood	Hemolysis assay	3.125 – 1600 μg/ml	3	Cell viability significantly decreases compared to control cells at NP sizes between 19 – 68 nm	[13]
Nonporous SiO	24 ± 3 nm	Human RBC and mast cells	Monitoring hemolysis and MTT	0 – 400 μg/ml	24	Cell viability decreased by 72% compared to control. Hemolysis at concentrations greater than 20 μg/ml	[116]
Mesoporous pSi microparticles	1,6 μm, 3 μm hemispherical	Mice RBC and macrophages	Monitoring hemolysis, proliferation and cytokines production	5-10 particles/cell	0-48	No hemolytic activity. No release of pro-inflammatory cytokines	[100]

Table 4

In vitro studies on the interactions of Si and SiO particles with macrophages.

Type of Particle	Size of Particle	Cells	Assay	Dosage	Treatment time (h)	Conclusions	Ref
pSi particles	3.2 μm – hemispherical	THP-1 Monocyte	ELISA – proinflammatory cytokine analysis	Ratio of 5:1 Particles:cell	72	No observed release of cytokines IL-6 and IL-8 for 48 hrs	[117]
pSi microparticles	3.2 μm – hemispherical	J774A.1 macrophages	MTT	Ratio of 10:1 Particles:cell	24 – 96	No observable change in cell proliferation compared to control	[101]
Hydrocarbonized pSi	97 nm to 10 – 25 μm	RAW 264.7 macrophages	MTT	15 – 250 μg/ml	24	Cytotoxicity observed for all sizes at concentrations greater than 50 μg/ml	[118]
SiO	30 nm	RAW 264.7 macrophages	MTS	10 – 1000 μg/ml	24	Toxic to RAW 264.7 at concentrations greater than 10 μg/ml	[119]
Si NPs	3 nm	RAW 264.7 macrophages	MTT	1 - 200 μg/ml	24 and 48	Cytotoxicity was induced at concentrations greater than 20 μg/ml	[111]
Amorphous SiO	7 – 300 nm	RAW 264.7 macrophages	MTT	0 – 1000 μg/ml	24	Size dependent effect: 50% cell viability decreased at 10 μg/ml for 7 nm NPs and at concentrations greater than 100 μg/ml for 300 nm	[120]
Amorphous SiO	22 nm	RAW 264.7 macrophages	Cell-Titer glow luminescent	10 – 500 μg/ml	24	No change in cell morphology	[121]
Si microparticles	100 – 3000 nm	RAW 264.7 macrophages	MTT	1 - 200 μg/ml	24 and 48	Cytotoxicity was induced at concentrations greater than 200 μg/ml	[111]
pSiO and SiO NPs	Nonporous SiO NPs (115 nm), mesoporous pSiO nanospheres (120 nm diameter, aspect ratio 1), mesoporous pSiO nanorods with aspect ratio of 2, 4, and 8 (width by length 80 × 200 nm, 150 × 600	RAW 264.7 macrophages	WST-8, ICP-MS	100, 250, or 500 μg/ml	24	Cellular association of the SiO NPs directly linked to the extent of plasma membrane damage. Effect charge/porosity dependent.	[109]

Adv Drug Deliv Rev. Author manuscript; available in PMC 2013 December 01.

Type of Particle	Size of Particle	Cells	Assay	Dosage	Treatment time (h)	Conclusions	Ref
	nm, 130 × 1000 nm), and their cationic counterparts						

Table 5

In vitro studies on the interactions of Si and SiO particles with epithelia cells.

Type of Particle	Size of Particle	Cells	Assay	Dosage	Treatment time (h)	Conclusions	Ref
SiO	20 – 760 nm	Human embryonic kidney (HEK293)	MTT	20 – 2000 μg/ml	24	Cells treated with 20 nm NP reduced cell viability by 50% at concentrations greater than 80 μg/ml compared to treatment with larger NP sizes, which decreased cell viability by 50% at concentrations greater than 140 μg/ml	[122]
pSiO	166 nm (diameter) and 320 nm (long)	Human neuroblastoma (SK-N-SH)	Trypan blue	40 – 800 μg/ml	48	Reduced cell viability by 50% compared to control at particle numbers greater than 5×10^{10}	[124]
pSi NPs	126 nm with pore diameters of 5 – 10 nm	HeLa (kidney epithelium)	MTT	0 – 0.2 mg/ml	48	Bare NPs showed no toxicity, but loaded doxorubicin NPs produced cytotoxicity at Doxorubicin concentrations greater than 1 μg/ml	[77]
SiO NPs	70 nm	HeLa	WST-1	50 μg/ml	24	In the presence of serum, not cytotoxic, but in the absence of serum, NPs were highly toxic	[125]
SiO NPs	200 and 500 nm	HeLa	WST-1	50 μg/ml	24	No toxicity observed with and without serum	[125]

Table 6

In vitro studies on the interactions of Si and SiO particles with lymphocytes, fibroblasts and other cells.

Type of Particle	Size of Particle	Cells	Assay	Dosage	Treatment time (h)	Conclusions	Ref
pSi	50 and 200 nm	B lymphoma A20 cell line	Flow cytometry analysis	Not specified	72	No evidence of secretion of inflammatory cytokines and change in cell morphology and viability	[126]
pSiO	31.5 Å (Pore width)	Human T-cell lymphoma (Jurkat) cells	WST-8	50 – 200 μg/ml	3 – 51	No cytotoxicity observed when functionalized with amines	[127]
pSiO	59.2 Å (pore width)	Human T-cell lymphoma (Jurkat) cells	WST-8	50 – 200 μg/ml	3 – 51	No cytotoxicity observed when functionalized with amines	[127]
Spherical amorphous SiO	10, 30, 80, and 400 nm	D3 murine embryonic stem cell	Embryonic stem cell test (EST), WST-1	10 - 1000μg/ml	24 hr, 5 days, 10 days	10 and 30 nm NPs inhibited differentiation of stem cells	[128]
SiO NPs	50 and 200 nm	Afeuronal cell line GT1-7	Crystal violet	15 – 292 μg/ml	24 and 72	50 nm NPs were cytotoxic at concentrations greater than 15 μg/ml and 200 nm NP were not cytotoxic at up to high concentrations of 292 μg/ml	[129]
SiO NPs	38 nm	3T3 fibroblasts	XTT	5 – 100 μg/ml	24	Cell viability decreased by 50% at SiO concentrations greater than 50 μg/ml	[130]
Spherical SiO microspheres	300 nm	Human T-cell lymphoma (Jurkat) cells	WST-8	50 – 200 μg/ml	3 μ 51	No inhibitory effect observed on cell growth	[127]
SiO	30 nm	3T3 fibroblasts	MTS	10 – 1000 μg/ml	24	30% decrease in cell viability compared to control at concentrations between 10 to 1000 μg/ml	[119]
pSiO	31.5 A (MCM – 41 Pore width), 59.2 (pore width – SBA-15), SMS – 300 nm	Human neuroblastoma: Sk-N-H cells	WST-8	50 – 200 μg/ml	3 – 51	Cell viability decreases by 20% compared to control for MCM-41 and SBA – 15 within 24 hours, whereas, SMS was not cytotoxic up to high concentrations of 200 μg/ml and long exposures up to 51 hrs	[127]

Table 7

In vivo studies on intravenous administration of Si and SiO particles.

Particle Type	Particle Size	Model	Evaluation	Dosage	Treatment time	Conclusions	Ref
SiO spheres	0.7, 1, 1.5, 2.53, and 5 urn	Nude rice	ICP-AES and histology	10^7 or 10^8 particles in 100 μl saline	4 hrs for 0.7 μm; 2 hrs for 1 – 2.53 μm	As diameter decreased, there was less deposition observed in non-RES organs	[134]
Non-spherical pSiO	1 and 1.5 μm	Nude rice	ICP-AES and histology	10^8 particles in 100 μl saline	6 h	Large accumulation was observed in most of the organs (liver, spleen, lungs, kidneys)	[134]
Mesoporous pSiO NPs	80 – 360 nm	ICR mice	Histology	20 mg/kg	Up to 1 month	NPs found mainly in liver, and spleen and little in kidney and heart. No tissue toxicity after 1 month in vivo	[135]
Mesoporous hollow pSiO NPs	110 nm	ICR mice	ICP-OES	20 – 80 mg/kg	Up to 4 weeks	Low toxicity observed with single and repeated administration; NPs mainly accumulated by mononuclear phagocytic cells in liver and spleen. 100% Clearance took over 4 weeks.	[136]
Mesoporous pSiO NPs	Aspect ratio (1.5 and 5)	ICR mice	ICP-OES and histology	20 mg/kg	2h, 24 h, 7 days	NPs present in liver, spleen, and lung. Short rods were trapped in liver, Long rods in spleen. Excreted by urine and feces. Short rods have more rapid clearance. No toxicity observed, but maybe biliary excretion and glomerular filtration dysfunction	[14]
Hydrocarbonized pSi	1 – 10 and 10- 25	Winstar Han rats	Radioactivity measured with a gamma counter	Not specified	30 min to 6 hr	NPs mainly found in liver and spleen (rapid clearance)	[137]
pSi NPs	50 and 200 nm	Balb/c mice	Histology	1.6×10^{12} nanoparticles	72 h	No systemic toxicity observed	[126]
pSi NPs	126 nm with pore diareters of 5 – 10 nm	Nude mouse	ICP-OES	20 mg/kg	4 weeks	NPs accumulate mostly in the liver and spleen. Accumulation was mostly cleared by 1 week and completely by 4 weeks.	[77]
SiO NPs	20 and 80 nm	ICR mice	Histological	1 mg/ml	Up to 30 days	NPs accumulated mostly in the liver and spleen and retained in these tissues for over 30 days. There was lymphocytic infiltration at the portal area and	[110]

Particle Type	Particle Size	Model	Evaluation	Dosage	Treatment time	Conclusions	Ref
						hepatocyte necrosis in the liver	
SiO NPs	30, 70, 300 nm	BALB/c mice	Gas chromatography-mass spectrometry	10, 40, and 200 mg/kg, respectively	3 hr and 24 h	No differences by sizes among the metabolite profiles; energy metabolism, amino acid metabolism, lipid metabolism, and nucleotide metabolism may have cause hepatotoxicity	[132]
SiO NPs	20 – 25 nr	Athymic nude mice	Fluorescence and histology	2 mg/kg	Up to 15 days	Large accumulation in liver, spleen, and stomach than in kidney, heart, and lungs. Evidence of hepatobiliary excretion. no observed systemic toxicity	[138]
SiO	100 and 200 nm	BALB/c mice	Histopathology and Immuno-fluorescence staining	50 mg/kg	12 h, 24, 48, 72 h, and 7 days	200 nm were internalized faster than 100 nm by macrophages of spleen and liver	[139]
pSi	1.6 μm	FBV male and female mice	Histological, LDH	10^7,10^8 and 5×10^8 particles in 100 μL saline	1 day, 4 weeks	No change in blood chemistry and cytokines profile.	[81]
pSiO	500-1000 nm	Pregnant rats	Evaluation of transplacental passage	10^9 particles in 1000μL saline	4-24 hours	Size dependent penetration across placenta	[140]

Adv Drug Deliv Rev. Author manuscript; available in PMC 2013 December 01.

Table 8

In vitro studies on the interactions with Si and SiO particles on lung cells

Particle Type	Particle Size	Cells	Assay	Dosage	Treatment time (h)	Conclusions	Ref
Ultrafine amorphous SiO	14 nm	Alveolar type II epithelial cells	Gap junctional intercellular assay	10 μg/ cm^2	24	Gap junctional intercellular communication decreased by 77 % compared to control	[147]
Fine amorphous SiO	< 5μm	Alveolar type II epithelial cells	Gap junctional intercellular assay	10 μg/ cm^2	24	Gap junctional intercellular communication decreased by 59 % compared to control	[147]
SiO	10 and 80 nm	Human epithelial lung cells (A549)	Lactate dehydrogenase (LDH) assay	100 μg/ml	48	Cell viability decreased by 10% compared to control for both NP sizes at concentrations greater than 100 μg/ml	[148]
Amorphous SiO	15 and 46 nm	A549	Sulforhodamine B (SRB) assay	0 – 100 μg/ml	24 – 72	Cell viability decreased by 25% compared to control for both NP sizes at concentrations greater than 50 μg/ml	[149]
Amorphous SiO	~ 29.3 nm	A549	MTT	50 and 150 μg/ml	24	Cell viability decreased by 50% compared to control for both NP sizes at concentrations greater than 50 μg/ml	[150]
Crystalline and amorphous SiO	1600 nm (crystalline), 1000 – 3000 nm (amorphous)	Rat L2 lung epithelial cells	MTT, LDH	0.052 – 520 μg/cm^2	4 – 48	Within 24 hrs, LDH release increased both crystalline and amorphous particles at dose concentrations greater than 5.2 μg/cm^2	[151]
SiC	13 – 58 nm	A549	MTT	1 – 200 μg/ml	24	Cell mortality increased by 10 % compared to control at dose concentrations of 1 μg/ml within 24 hrs. minimal toxicity was observed overall	[152]
SiO	30 nm	hT, bronchiolar epithelial cells	MTS	10 – 1000 μg/ml	24	Cellular toxicity was observed at concentrations of greater than 100 μg/ml	[119]
SiO	115 nm	A549	ICP-MS, WST-1	Up to 500 μg/ml	24	Cellular toxicity was not observed compared to control	[14]
Amorphous SiO	10 – 20 nm	A549	MTT	5 – 200 μg/ml	4 – 48	Cellular toxicity was not observed compared to control	[153]

Table 9

In vivo studies on inhaled Si and SiO particles.

Particle Type	Particle Size	Model	Evaluation	Dosage	Treatment time	Conclusions	Ref
Amorphous SiO	37 or 83 nm	(SD) IGS BR rats	Histopathology	$10^7$to 10^8 particles/cm^3 (equivalent dosage of 1.8 or 86 mg/m^3)	1 and 3 days	No significant pulmonary inflammatory, genotoxic, or adverse lung histopathological effects observed	[155]
Crystalline SiO	1600 nm	(SD)IGS BR rats	Bronchoalveolar lavage (BAL)	1 to 5 mg/kg	24 h, 1 week, 1 month and 3 months	% polymorphonuclear leukocytes observed after exposure to particles increased	[151]
Amorphous SiO	1000 – 3000 nm	(SD)IGS BR rats	BAL	1 to 5 mg/kg	24 h, 1 week, 1 month and 3 months	Observed reversible and transient inflammatory responses	[151]
SiO (α-quartz structure)	50 nm	(SD)IGS BR rats	Histopathology	1 or 5 mg/kg	24 hrs, 1 week, 1 month, and 3 months	Acute lung inflammatory observed at 24 hrs	[156]
SiO (α-quartz structure)	300 - 700 nm	(SD)IGS BR rats	Histopathology	1 or 5 mg/kg	24 hrs, 1 week, 1 month, and 3 months	Persistent lung inflammatory observed at all time points	[156]
SiO (α-quartz structure)	12 nm	(SD)IGS BR rats	Histopathology	1 or 5 mg/kg	24 h, 1 week, 1 month, and 3 months	Persistent lung inflammatory observed at all time points	[156]
SiO (α-quartz structure)	300 nm	(SD)IGS BR rats	Histopathology	1 or 5 mg/kg	24 h, 1 week, 1 month, and 3 months	Fine quartz produced low inflammatory response compared to Min-U-Sil and Nanoquartz II	[156]
pSiO (MCM41-cal)	300 – 1000 nm	Balb/c mice	Immuno-histochemistry	200 μg/ml	5 – 14 h	No difference in the number of apoptotic cells compared to control	[154]
pSiO (SBA15 – cal)	Rods (d= 500 nm; l= 1000 nm)	Balb/c mice	Immuno-histochemistry	200 μg/ml	5 – 14 h	No difference in the number of apoptotic cells compared to control	[154]
SiO	10 nm	Wistar rats	Histological analysis	100 and 300 μg/ml	24 h	No observed inflammation in the lungs	[139]
Ultrafine	14 nm	ICR mice	Histopathology and BAL	0 – 100 μg/ml	3 days	Exposure of 30 ug produced moderate to severe pulmonary inflammation and tissue injury at acute periods and an apoptotic	[157]

Particle Type	Particle Size	Model	Evaluation	Dosage	Treatment time	Conclusions	Ref
						increase in lung parenchyma and oxidative stress	

Table 10

In vitro, ex vivo and in vivo studies related to skin application of Si and SiO based particles.

Particle Type	Particle size, nm	Biological System	Assay/Model	Treatment Time, h	Dosage (μg/ml)	Conclusions	Ref.
SiO	7 or 10 – 20	*In vitro*- HaCaT human keratinocytes	MTT	48	30 - 300	Cell viability slightly decreases by 10% compared to control at a concentration of 50 μg/ml	[164]
SiO	7 or 10 – 20	*In vitro* – 3D EpiDerm™ Skin Model	MTT	5 and 18	500	No observed difference in cell viability compared to control cells	[164]
SiO	80	*In vitro* – human dermal fibroblasts	MTT, Cell adhesion assay	24	100	Decrease in cell viability at concentrations greater than 50 μg/ml; weakened the mitochondrial membrane potential. Cell adhesion and migration was affected	[165]
SiO	500	*In vitro* – human dermal fibroblasts	MTT, cell adhesion assay	24	100	No observed difference in cell viability compared to control cells	[165]
SiO	70	*In vitro* – HaCaT human keratinocytes	LDH Cytotoxicity assay	24	< 10	LDH release increased at concentrations greater than 250 μg/ml	[167]
SiO	300 and 1000	*In vitro* – HaCaT human keratinocytes	LDH Cytotoxicity assay	24	< 10	No significant change in LDH release observed up to concentrations of 1250 μg/ml	[167]
SiO	10-80	*In vitro* – adherent fibroblast - WS1 and CCD-966sk	MTT	48	Various	20% cell viability for WS1 decreased at dosage concentrations greater than 171 μg/ml and for CCD-966sk decreased at dosage concentrations greater than 224 μg/ml. Observed retardation of cell proliferation and damage to cell membrane.	[52]
SiO	3000	*Ex vivo* - Dermatomed human skin	Scanning Electron Microscope	24	0.1% (w/v) in 500 μL	Particles were observed to penetrate through the epidermis	[168]
Gold particles coated with SiO shell	95, 160	*Ex vivo* – patient samples from plastic surgery	Scanning transmission x-ray microscopy	1.5	1000 – 4000	Particles (161 nm) spread on the superficial layer of the stratum corneum and on the epithelium in superficial parts of hair follicles	[169]

Particle Type	Particle size, nm	Biological System	Assay/Model	Treatment Time, h	Dosage (μg/ml)	Conclusions	Ref.
SiO	7 or 10 – 20	*In vivo* - (Rabbits)	Draize Patch skin irritation Test	24 and 72	Not specified	No observable edema or erythema and skin irritation	[164]